Plasma MicroRNA Profiling of *Plasmodium falciparum* Biomass and Association with Severity of Malaria Disease

Himanshu Gupta,[1,2] Mercedes Rubio,[1] Antonio Sitoe, Rosauro Varo, Pau Cisteró, Lola Madrid, Inocencia Cuamba, Alfons Jimenez, Xavier Martiáñez-Vendrell, Diana Barrios, Lorena Pantano, Allison Brimacombe, Mariona Bustamante, Quique Bassat,[3] Alfredo Mayor[3]

Severe malaria (SM) is a major public health problem in malaria-endemic countries. Sequestration of *Plasmodium falciparum*–infected erythrocytes in vital organs and the associated inflammation leads to organ dysfunction. MicroRNAs (miRNAs), which are rapidly released from damaged tissues into the host fluids, constitute a promising biomarker for the prognosis of SM. We applied next-generation sequencing to evaluate the differential expression of miRNAs in SM and in uncomplicated malaria (UM). Six miRNAs were associated with in vitro *P. falciparum* cytoadhesion, severity in children, and *P. falciparum* biomass. Relative expression of hsa-miR-4497 quantified by TaqMan-quantitative reverse transcription PCR was higher in plasma of children with SM than those with UM ($p<0.048$) and again correlated with *P. falciparum* biomass ($p = 0.033$). These findings suggest that different physiopathological processes in SM and UM lead to differential expression of miRNAs and pave the way for future studies to assess their prognostic value in malaria.

Author affiliations: ISGlobal, Hospital Clinic—Universitat de Barcelona, Barcelona, Spain (H. Gupta, M. Rubio, R. Varo, P. Cisteró, A. Jimenez, X. Martiáñez-Vendrell, D. Barrios, A. Brimacombe, M. Bustamante, Q. Bassat, A. Mayor); Centro de Investigação em Saúde de Manhiça (CISM), Maputo, Mozambique (A. Sitoe, R. Varo, L. Madrid, I. Cuamba, Q. Bassat, A. Mayor); Spanish Consortium for Research in Epidemiology and Public Health (CIBERESP), Madrid, Spain (A. Jimenez, M. Bustamante, Q. Bassat, A. Mayor); Harvard T.H. Chan School of Public Health Department of Biostatistics, Boston, Massachusetts, USA (L. Pantano); Universitat Pompeu Fabra (UPF), Barcelona (M. Bustamante); Institut Català de Recerca en Estudis Avançats (ICREA), Barcelona (Q. Bassat); Hospital Sant Joan de Déu—University of Barcelona Pediatrics Department, Barcelona (Q. Bassat)

DOI: https://doi.org/10.3201/eid2702.191795

Case-fatality rates for *Plasmodium falciparum* severe malaria (SM) remain unacceptably high in young children in Africa (*1*). Early detection and prompt treatment of SM are critical to improve the prognosis of sick children. Unfortunately, clinical signs and symptoms in many malaria patients, particularly early in the infection, may not adequately indicate whether the infection will trigger severe or life-threatening disease. Moreover, in malaria-endemic areas, where immunity to malaria is progressively acquired, detecting peripheral *P. falciparum* parasitemia in sick children does not necessarily prove that malaria is the cause of the severe pathology observed, given that many persons may carry parasites without expressing clinical malarial disease (*2*).

Sequestration of *P. falciparum*–infected erythrocytes (iEs) (*3*) in vital organs is considered a key pathogenic event leading to SM, as has been shown in postmortem parasite counts in patients who died with cerebral malaria (*4,5*). This extensive sequestration of parasitized erythrocytes in the microvasculature, together with the production of inflammatory mediators, leads to the dysfunction of one or more peripheral organs, such as the lungs (acute respiratory distress syndrome), kidneys (acute kidney injury) or brain (coma) (*6,7*). This tissue-specific tropism of *P. falciparum* parasites is mediated by the *P. falciparum* erythrocyte membrane protein 1 (PfEMP1), which can bind to different host receptors on the capillary endothelium, uninfected erythrocytes, and platelets (*8,9*); such receptors include endothelial receptor of

[1]These authors contributed equally to this article.

[2]Current affiliation: London School of Hygiene and Tropical Medicine, London, UK.

[3]These senior authors contributed equally to this article.

protein C (ePCR), gC1qR, intercellular adhesion molecule-1, CD36, chondroitin sulfate A, or complement receptor 1 (*10*).

Efforts have been made to identify biomarkers of SM that could be used for early diagnosis and for reducing severity of disease (*11*). Several biomarkers related to endothelial activation and immune dysfunction have been associated with different malaria-derived severe pathologies (*11–14*). Plasma level of histidine-rich protein 2 (HRP2), a parasite-specific protein secreted by the parasite during its blood cycle, has been used as a biomarker of total parasite biomass (circulating and sequestered parasites) (*15,16*) and therefore as a prognostic marker of the total parasite biomass and as a better proxy marker for SM than peripheral parasitemia (*16*). Organ damage and pathological disease states have also been associated with the rapid release of microRNAs (miRNAs), a class of endogenous small noncoding RNAs (18–24 nt), into circulation (*17*). Because secreted miRNAs can be detected in biologic fluids such as plasma (*18*), they are currently being explored (*17*) as promising noninvasive biomarkers to monitor organ functionality and tissue pathophysiological status. The content of miRNAs in the host is influenced by host-pathogen interactions (*19*). Sequestration of erythrocytes infected with *P. berghei* in mice brains has been demonstrated to modify the miRNA expression in cells (*20*). Similarly, sequestration of *P. vivax* gametocytes in bone marrow has been associated with transcriptional changes of miRNAs involved in erythropoiesis (*21*). The evidence suggests that *Plasmodium* parasites, although unable to produce miRNAs (*22*), could affect the production of organ-specific host miRNAs, pointing toward the potential of these small molecules to detect SM associated organ injury (*23*) and to confirm the contribution of malaria in the chain of events leading to death through the analysis of postmortem tissues (*23*).

Our study hypothesis is that miRNA levels in plasma are differentially expressed among children with severe and uncomplicated malaria because of the parasite sequestration in vital organs of severely ill children. To identify promising biomarkers for SM, we conducted a small RNA next-generation sequencing study to select miRNAs that were differentially expressed by human brain endothelial (HBE) cells exposed to *P. falciparum* iEs selected for cytoadhesion to ePCR, the main host receptor associated with SM (*9*), compared with HBE cells exposed to noncytoadherent iEs and noninfected erythrocytes (niEs). We also compared children who had SM with children who had UM (Figure 1). miRNAs that were differentially expressed in both analyses, together with the *P. falciparum* biomass-associated miRNAs (correlation coefficient >0.50 [*24*]), were quantitatively confirmed in

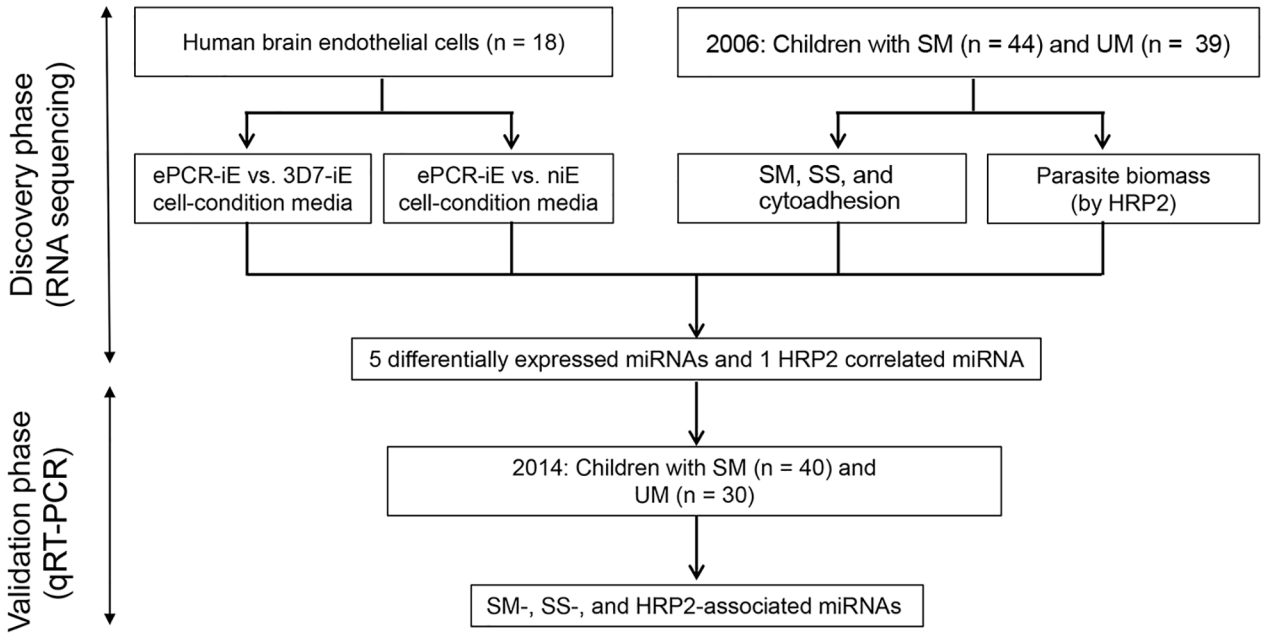

Figure 1. Schematic representation of study design to identify miRNA-based biomarkers of SM. ePCR, endothelial protein-C receptor (a binding *Plasmodium falciparum* strain-FCR3); HRP2, histidine-rich protein 2; iE, infected erythrocyte; miRNA, microRNA; niE, noninfected erythrocyte; SM, severe malaria; SS, severity symptoms; UM, uncomplicated malaria; 3D7, a nonbinding *P. falciparum* strain.

an independent validation cohort set of children with SM and UM using TaqMan quantitative reverse transcription PCR (qRT-PCR).

Materials and Methods

Study Population

Plasma samples used to assess miRNA levels were collected in 2 case–control studies conducted in Manhiça District in southern Mozambique during 2006 (n = 113) and 2014 (n = 91). In brief, the cases were children <5 years of age admitted to Manhiça District Hospital for SM and controls were outpatient children with UM (Appendix, https://wwwnc.cdc.gov/EID/27/2/19-1795-App1.pdf). The National Mozambican Ethical Review Committee (Mozambique) and Hospital Clínic (Barcelona, Spain) approved study protocols for each of the case–control studies. A signed written informed consent was obtained from each participant's guardian or parent during the original studies.

Parasitological Determinations

We prepared thick and thin blood films to quantify *P. falciparum* parasitemia. We used approximately half of a 60µL dried blood drop on Whatman-903 filter paper to extract parasite DNA and performed real-time quantitative PCR (qPCR) targeting the *P. falciparum* 18S rRNA gene (*25,26*). HRP2 levels were quantified using commercially available ELISA kits and an in-house highly sensitive quantitative bead suspension array (qSA) based on Luminex technology (Appendix).

P. falciparum Cytoadhesion Assays

We performed cytoadhesion assays to discover the differential expression of miRNAs (Appendix). HBE cells were incubated with *P. falciparum* iEs at the trophozoite stage of the ePCR binding FCR3 strain (ePCR-iE, which expresses the PfEPM1 protein that binds to ePCR receptor) and the 3D7 strain (3D7-iE, a strain without the protein that binds to ePCR receptor). Noninfected erythrocytes were used as negative control. The cell-conditioned media of each group were collected after 1 h (t1) and 24 h of stimulation (t24) and subjected to RNA extraction followed by small-RNA sequencing.

Molecular Procedures, Gene Target Prediction and Data Analysis

RNA was extracted from cell-conditioned media (3 mL) by using the miRNeasy tissues/cells kit (QIAGEN, https://www.qiagen.com) and from plasma samples (1 mL) by using the miRNeasy plasma/serum kit, with the use of 5µg UltraPure glycogen/sample. Given that the plasma samples were conserved in heparin, RNA was precipitated with lithium chloride as described previously (*27*). Purified RNA was subjected to library preparation, pooling, and sequencing using a HiSeq 2000 (Illumina, https://www.illumina.com) platform, following the protocol for small RNAs (*28*) (Appendix). We used a previously published pipeline (*28*) to assess the sequencing quality, identification, and quantification of small RNAs, normalization and other species RNA contamination (Appendix). To detect miRNAs and isomiRs, reads were mapped to the precursors and annotated to miRNAs or isomiRs using miRBase version 21 with the miraligner (*29*). DESeq2 R package version 1.10.1 (R3.3.2; https://www.r-project.org/about.html) (*30*) was used to perform an internal normalization.

In the 2014 study, we used 50 µL of plasma with no hemolysis for RNA extraction as described, then conducted qRT-PCR (Appendix). We calculated miRNA relative expression levels (RELs) by the $2^{-\Delta C_t}$ method, where ΔC_t = cycle threshold (C_t) (miRNA) – mean C_t (endogenous controls; ECs), considering efficiencies of 100% for all the miRNAs and ECs (*31*).

The selected miRNAs were screened through different gene target prediction programs such as DIANA-microT-CDS (http://www.microrna.gr/microT-CDS), MiRDIP (http://ophid.utoronto.ca/mirDIP), MirGate (http://mirgate.bioinfo.cnio.es), and TargetScan (http://www.targetscan.org) (Appendix). We assessed differential expression of miRNAs and isomiRs using DESEq2 and IsomiRs packages in R (*29,32*) (Appendix). All statistical analyses were performed using R version 3.3.2, and graphs were prepared with GraphPad version 6 (https://www.graphpad.com).

Results

Discovery Phase

miRNA Expression by HBE Cells

The ePCR binding *P. falciparum* strain (FCR3; ePCR-iE) showed higher levels of cytoadhesion to HBE cells (mean 32.60, SD 4.87 iE/500 cells) than a nonbinding *P. falciparum* (3D7; 3D7-iE) strain (mean 3.20, SD 1.06 iE/500 cells; p = 0.001) and noninfected erythrocytes (mean 3.12, SD 0.39 iE/500 cells; p = 0.001) (Appendix Figure 1). We sequenced 3 replicates of the media collected from each cytoadhesion assay after 1 h (t1) and 24 h (t24), giving a total of >200 million reads/lane, with a mean of 12.10 million reads (SD 13.31) per sample (Table 1; Figure 2, panel A; Appendix Table

Table 1. Quality control and mapped reads in different species of small RNAs from cell-conditioned media of human brain endothelial cells and plasma samples in children with uncomplicated and severe malaria, Mozambique*

	Cell condition							
	niE		3D7-iE		ePCR-iE			
Read type	t1, n = 3	t24, n = 3	t1, n = 3	t24, n = 3	t1, n = 3	t24, n = 3	UM, n = 39	SM, n = 44
Total reads, millions (SD)	8.70 (3.55)	16.71 (14.59)	10.43 (3.48)	25.86 (28.14)	4.78 (2.13)	6.11 (1.18)	10.90 (9.69)	9.26 (6.06)
Quality filtered, counts (SD)	46.00 (36.72)	33.33 (29.67)	14.67 (23.69)	125.67 (217.66)	10.67 (2.31)	16.33 (25.70)	557.62 (1,200.76)	615.75 (1,163.62)
Complexity filtered, counts (SD)	910.67 (775.48)	745.00 (659.60)	369.33 (567.40)	3168.67 (5,438.11)	220.67 (163.57)	308.00 (526.55)	535.97 (884.46)	506.23 (455.16)
Size filtered, millions (SD)	0.63 (0.34)	2.26 (2.99)	0.68 (0.40)	2.12 (2.92)	0.90 (0.48)	0.49 (0.50)	1.94 (1.51)	2.39 (1.82)
Good-quality reads†								
Millions (SD)	8.07 (3.35)	14.44 (11.60)	9.75 (3.10)	23.74 (25.23)	3.88 (2.00)	5.62 (0.84)	8.96 (8.89)	6.88 (4.64)
Percentage (SD)	92.62 (2.54)	90.35 (6.98)	93.93 (2.37)	94.15 (3.26)	79.60 (8.86)	92.62 (6.35)	77.76 (15.31)	74.95 (11.08)
miRNA								
Millions (SD)	0.26 (0.19)	1.09 (1.57)	0.27 (0.19)	0.98 (1.14)	0.25 (0.07)	0.15 (0.13)	2.05 (2.50)	1.33 (1.42)
Percentage (SD)	3.02 (1.73)	4.97 (4.92)	2.47 (1.52)	3.75 (0.54)	7.41 (3.44)	2.47 (1.97)	22.43 (16.01)	20.21 (13.22)
rRNA								
Millions (SD)	2.34 (1.82)	3.12 (2.71)	1.57 (1.72)	5.74 (9.19)	0.72 (0.38)	0.90 (1.08)	0.92 (0.97)	0.81 (0.72)
Percentage (SD)	24.72 (16.01)	20.36 (14.62)	14.84 (15.37)	13.41 (15.42)	19.55 (5.14)	15.13 (16.99)	11.11 (7.75)	11.49 (5.78)
tRNA								
Millions (SD)	1.72 (0.58)	3.37 (1.51)	3.75 (1.80)	6.35 (3.00)	0.84 (0.64)	2.47 (1.47)	1.13 (1.17)	1.14 (0.94)
Percentage (SD)	27.51 (23.37)	32.53 (27.16)	41.04 (20.74)	43.47 (23.59)	18.65 (9.43)	45.24 (26.80)	13.93 (6.85)	17.79 (7.70)
Unknown								
Millions (SD)	3.75 (1.92)	6.86 (6.80)	4.16 (1.67)	10.66 (12.55)	2.07 (0.97)	2.11 (0.67)	4.87 (5.88)	3.59 (2.62)
Percentage (SD)	44.76 (6.35)	42.14 (11.63)	41.65 (5.12)	39.37 (8.36)	54.40 (3.75)	37.15 (7.89)	52.53 (16.01)	50.51 (13.55)

*Reads were obtained from cell-conditioned media of human brain endothelial cells exposed to cytoadherent *P. falciparum*–infected and noninfected erythrocytes, and plasma of Mozambique children with SM and UM. Three replicates of the media were collected from each cytoadhesion assay after 1 (t1) and 24 (t24) hours. ePCR-iE, adherent FCR3 expression endothelial receptor of protein C-infected erythrocytes; miRNA, microRNA; niE, noninfected erythrocytes; SM, severe malaria; UM, uncomplicated malaria; 3D7-iE, nonadherent 3D7-infected erythrocytes.
†Reads after filtering low quality, low complexity, and short (<18-nt) sequences.

1). The mean percentage of miRNAs in the media samples analyzed was 4.01% (SD 2.93%); a mean of 203 (SD 93.82, range 101–465) distinct miRNAs were detected (Appendix Table 1). The 10 most expressed miRNAs for all samples at t1 and t24 time points are described in Figure 2, panel B. No contamination with RNA from other species was observed.

One hour after incubating the HBE cells with *P. falciparum* infected and noninfected erythrocytes, 111 miRNAs were found to be differentially expressed in cell-condition media of niE and ePCR-iE; 76 of them were downregulated and 35 upregulated in ePCR-iE compared with niE (Figure 2, panel C; Appendix Table 2). At this same time point, 100 miRNAs were differentially expressed in cell-condition media of 3D7-iE and ePCR-iE; 67 were downregulated and 33 upregulated in ePCR-iE compared with 3D7-iE (Figure 2, panel D; Appendix Table 3). Overall, 89 miRNAs were differentially expressed in ePCR-iE compared with both niE and 3D7-iE; 28 of those were upregulated and 61 downregulated in ePCR-iE. There were no differentially expressed miRNAs between niE and 3D7-iE cell-condition media. At t24, only hsa-miR-451a was significantly upregulated in cell-condition media of ePCR-iE with respect to niE ($p<0.001$) and 3D7-iE ($p = 0.023$). We found no significantly different miRNAs between niE and 3D7-iE cell-condition media. All differentially expressed isomiRs originated from the selected miRNAs; none of them presented any modifications in the seed region.

miRNAs Expression in Plasmas from Children with Malaria of Varying Severity

Out of 113 plasma samples collected from children with SM (N = 57) and UM (N = 56) in Mozambique in 2006, 11 samples were discarded, 5 because of hemolysis ($OD_{414}>0.2$) (*33*) and 6 because no peak was observed between 133–150 nt (typical size for miRNAs

plus library adaptors) on the bioanalyzer results after library preparation. Among the 102 sequenced samples (SM = 53, UM = 49), 19 samples (9 SM, 10 UM) were further excluded because of the low number of miRNA reads (<10,000 reads). In total, samples from 83 children (44 with SM and 39 with UM) were included in the analysis (Table 2).

The sequencing of the 83 plasma samples yielded a mean of 9.42 (SD 6.4) million reads per sample (Table 1; Figure 2, panel A; Appendix Table 4). The mean percentage of miRNAs per plasma samples was 20.5% (SD 13.2%), with a mean of 395 (SD 169, range 116–786) distinct miRNAs detected (Appendix Table 4). The total number of miRNAs detected across samples was 1,450. The 10 most expressed miRNAs can be found in Figure 2, panel B. No contamination with RNA from other species was observed.

We found hsa-miR-122–5p upregulated in children with SM (Table 3). In the subanalysis by signs of severity, 5 miRNAs were associated with severe anemia (SA), prostration, and acute respiratory distress (ARD) (Table 3). Twelve miRNAs were associated

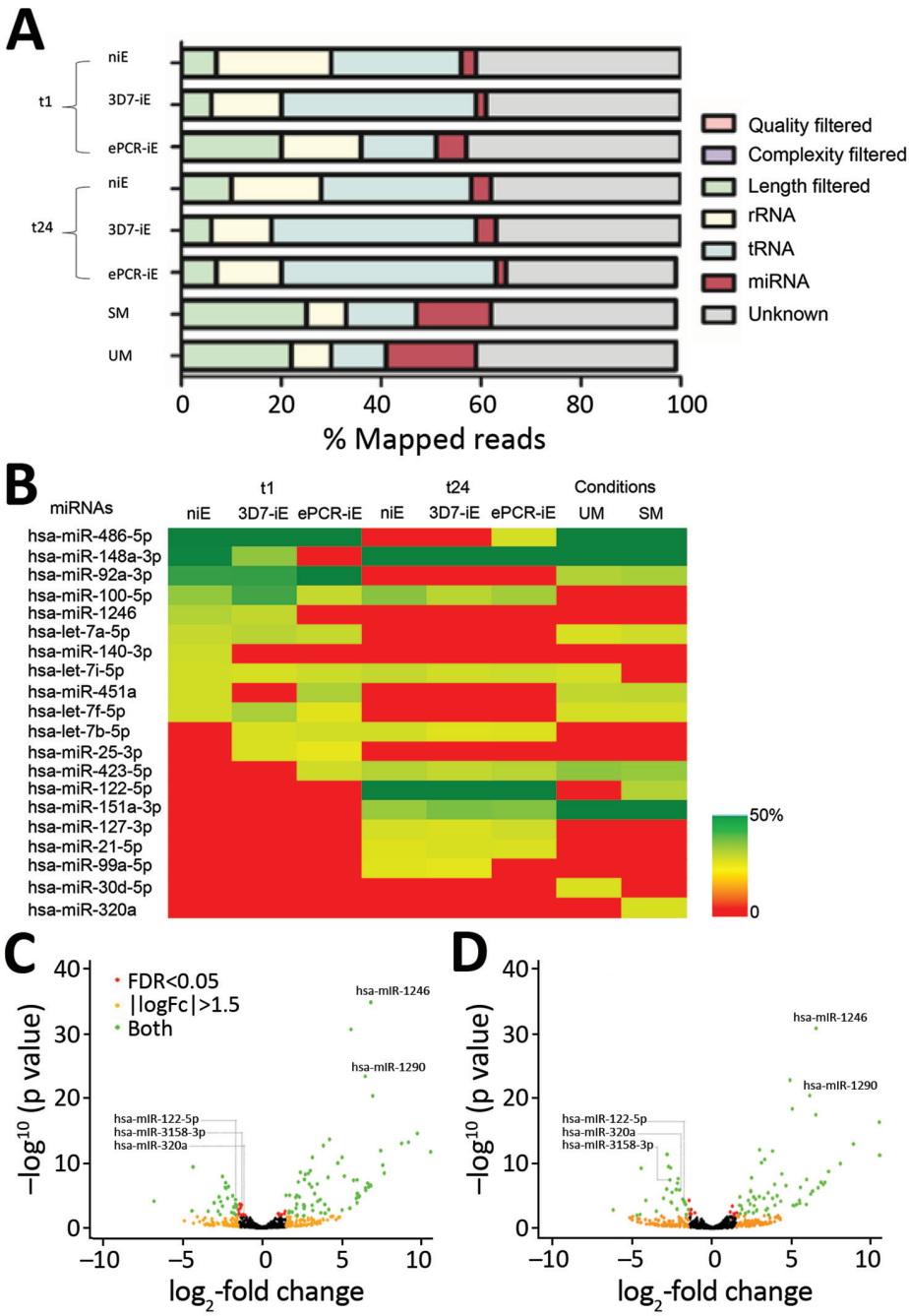

Figure 2. RNA sequencing of human brain endothelial (HBE) cell media and plasma from children recruited in 2006, Mozambique. A) Percentage of mapped reads in different species of small RNAs, for both in vitro and ex vivo approaches. B) Ten most expressed miRNAs in HBE cell medias and plasmas. Color-coded cells show the percentage of each assay/condition (columns) for each miRNA (rows). C) Volcano plot of differentially expressed miRNAs in cell-condition media of niEs versus cell-condition media of iEs with the FCR3-ePCR strain (ePCR-iE) incubated with HBE cells. D) Volcano plot of differentially expressed miRNAs in cell-condition media of iEs with 3D7 strain (3D7-iE) versus cell-condition media of iEs with the FCR3-ePCR strain (ePCR-iE) incubated with HBE cells. Comparisons depicted in C and D were adjusted for multiple testing by the Benjamini-Hochberg method. Negative $\log_2$-fold change indicates overexpression in ePCR-iE samples. ePCR, endothelial protein-C receptor (a binding *Plasmodium falciparum* strain); HRP2, histidine-rich protein 2; iE, infected erythrocyte; miRNA, microRNA; SM, severe malaria; UM, uncomplicated malaria.

Table 2. Characteristics of children with severe and uncomplicated malaria recruited for case–control studies in 2006 and 2014, Mozambique*

Characteristic	2006			2014		
	UM, n = 39	SM, n = 44	p value	UM, n = 30	SM, n = 40	p value
Age, y, mean (SD)†	2.3 (1.1)	2.4 (1.3)	0.671	2.2 (1.3)	2.8 (1.2)	0.419
Sex, no. (%)						
M	24 (62)	28 (64)	1.000	18 (60)	21 (52.5)	0.532
F	15 (38)	16 (36)		12 (40)	19 (47.5)	
HRP2, ng/mL, GM (SD)	71.3 (10.7)	331.4 (40.7)	<0.001	24.1 (4.9)	78.7 (12.2)	0.038
qPCR, parasites/µL, GM (SD)	2,084.9 (302.5)	7,976.1 (1,079.6)	0.004	72,845.9 (7,193.9)	94,099.6 (8,716.0)	0.549
Splenomegaly, no. (%)						
No	33 (85)	21 (48)	0.001	ND	27 (67.5)	NA
Yes	6 (15)	23 (52)		ND	13 (32.5)	
Hepatomegaly, no. (%)						
No	38 (97)	35 (80)	0.016	ND	35 (87.5)	NA
Yes	1 (3)	9 (20)		ND	5 (12.5)	
Hyperlactatemia, no. (%)						
No	10 (26)	5 (11)	0.152	26 (86.7)	27 (67.5)	0.064
Yes	29 (74)	39 (89)		4 (13.3)	13 (32.5)	
Temperature, ºC, mean (SD)	38.0 (1.6)	38.5 (1.1)	0.093	38.0 (1.3)	38.2 (1.4)	0.437
Weight, kg, mean (SD)	11.3 (2.8)	11.0 (2.8)	0.599	12.3 (2.9)	12.7 (3.3)	0.476
Platelets, 10^9/L, mean (SD)	156.7 (86.8)	115.8 (66.8)	0.018	149.0 (89.7)	95.3 (69.3)	0.001
Glucose, mM, mean (SD)‡	6.2 (1.5)	5.9 (1.8)	0.391	6.6 (1.3)	6.0 (2.6)	0.165
WBC, 10^9/L, mean (SD)	9.9 (4.1)	10.2 (3.9)	0.774	9.7 (3.8)	9.6 (5.0)	0.929
Neutrophils, %, mean (SD)§	54.1 (16.7)	54.4 (14.3)	0.940	50.7 (20.6)	58.9 (13.7)	0.447
Lymphocytes, %, mean (SD)¶	39.4 (17.9)	36.3 (12.6)	0.374	26.1 (17.1)	25.6 (12.2)	0.995
Lactate, mM, mean (SD)	3.0 (1.7)	4.7 (3.6)	0.009	2.8 (2.2)	3.6 (2.4)	0.035
Severe malaria syndromes, no. (%)						
Prostration		33 (75.0)			30 (75.0)	
Acute respiratory distress		18 (40.9)			19 (47.5)	
Severe anemia		17 (38.6)			7 (17.5)	
Multiple seizures		11 (25.0)			24 (60.0)	
Cerebral malaria		2 (4.5)			7 (17.5)	
Hypoglycemia		2 (4.5)			2 (5.0)	

*Data were gathered in a discovery study in 2006 and validation study in 2014. GM, geometric mean; HRP2, histidine-rich protein 2: NA, not applicable; ND, not determined; SM, severe malaria; UM, uncomplicated malaria; WBC, white blood cells.
†No data for 1 sample (UM = 1) in 2014 study.
‡No data for 3 samples (SM = 2; UM = 1) in 2014 study.
§No data for 4 samples (SM = 4) in 2014 study.
¶No data for 3 samples (SM = 3) in 2014 study.

with PM-agglutination and cytoadhesion to g1CqR (Table 3). We observed no associations between miRNA counts and other cytoadhesion data such as rosetting and binding to CD36 and to CD54. After adjusting for multiple comparisons, we found 3/1,450 miRNAs identified in RNA sequencing data, hsa-miR-10b-5p, hsa-miR-378a-3p, and hsa-miR-4497, correlated with HRP2 levels determined by qSA Spearman analysis (Figure 3). We observed similar correlations when HRP2 levels were determined by ELISA (Appendix Table 5). miRNAs were neither associated with hepatomegaly nor with splenomegaly. All differentially expressed isomiRs between children with SM and those with UM belong to the differentially expressed miRNAs, with no modifications in the seed region.

Validation Cohort

Among the 89 miRNAs differentially expressed in cell-condition media of HBE cells exposed to niE and 3D7-iE compared with ePCR-iE, we confirmed 5 miRNAs to be differentially expressed between children with SM and UM. These 5 miRNAs (hsa-miR-122–5p, hsa-miR-320a, hsa-miR-1246, hsa-miR-1290 and hsa-miR-3158–3p), along with hsa-miR-4497 miRNA, which had a correlation coefficient with HRP2 >0.5 (Figure 3), were selected for TaqMan qRT-PCR validation in an independent cohort of children with SM and UM recruited in 2014. Among the 91 plasma samples collected from these children, 21 were discarded because of hemolysis (OD_{414}>0.2) (*33*). Of the 70 remaining samples, 40 were collected from children with SM and 30 from children with UM (Table 2).

All samples tested by qRT-PCR amplified the exogenous control (ath-miR-159a) with a C_t value<18 and a coefficient of variance (CV) <5%, suggesting the correct RNA extraction and cDNA preparation. We selected 3 ECs, hsa-miR-191–5p (CV = 4.8%, baseMean = 3953.3, $\log_2$-fold change [FC] −0.02, SD 0.56), hsa-miR-30d-5p (CV = 4.9%, baseMean = 14172.31, FC 0.01, SD 0.61), and hsa-miR-148a-3p (CV = 5%,

baseMean = 111593.08, FC 0.11, SD 0.82) as a panel for qRT-PCR analysis. Among these, the NormFinder stability value was 0.044 for the combination of hsa-miR-30d-5p and hsa-miR-191–5p, and thus we selected those 2 ECs. No statistically significant differences were found when we compared C_t values of the exogenous controls and 2 endogenous controls between SM and UM samples (Appendix Figure 2). We performed standard curves for all miRNAs (ECs and selected miRNAs), giving efficiencies of 91.1%–103.8% (Appendix Table 6), which were assumed as 100% to calculate the relative expression values using the $2^{-\Delta C_t}$ method (*31*).

The relative expression levels of hsa-miR-3158–3p and hsa-miR-4497 were significantly higher in children with SM than UM ($p<0.05$) (Figure 4). We found that hsa-miR-3158–3p levels were higher in children who had prostration, multiple seizures, and ARD compared with those who had UM ($p<0.05$; Figure 5). Severe anemia and ARD symptoms were associated with higher hsa-miR-4497 levels ($p<0.05$; Figure 5). No such associations were observed for cerebral malaria and hypoglycemia. RELs of hsa-miR-3158–3p and hsa-miR-4497 were found positively correlated with HRP2 levels quantified by qSA ($p<0.05$; Figure 6). Similar correlations were observed when HRP2 levels were determined by ELISA (Appendix Table 5).

miRNA Gene Target Prediction

We identified a total of 87 putative targets for hsa-miR-3158–3p and hsa-miR-4497 miRNAs, none of which were shared by both miRNAs (Appendix Table 7). We predicted 45 experimentally validated mRNA targets for hsa-miR-3158–3p and 42 for hsa-miR-4497; the predicted targets were found to be involved in a broad range of biologic processes (Appendix Table 8). However, significance was lost when adjusted by the Benjamini-Hochberg method; none of the target genes were clustered under the KEGG pathway with $p<0.05$.

Discussion

Because of their specificity to cell type (*17*), microRNAs can reflect disease states and organ damage. Consequently, they have the potential to provide a new screening method for early detection of pathological *P. falciparum* sequestration and could become an effective prognosis tool for severe malaria.

Table 3. Association of miRNA levels with severe malaria, symptoms of severity, and *Plasmodium falciparum* cytoadhesion among children with uncomplicated and severe malaria, Mozambique*

Characteristic	miRNA	baseMean	log_2-fold change	Adjusted p value
Clinical data				
SM, n = 44 vs. 39 UM				
All	hsa-miR-122-5p	19,929.69	1.67	0.001
SA, n = 17 vs. 39 UM				
	hsa-miR-4492	17.34	2.81	0.046
	hsa-miR-4497	293.66	2.18	0.046
Prostration, n = 33 vs. 39 UM				
	hsa-miR-122-5p	20,677	1.89	0.001
	hsa-miR-6087	5.36	2.39	0.033
	hsa-miR-511-5p	126.67	1.36	0.040
Acidosis or respiratory distress, n = 18 vs. 39 UM				
	hsa-miR-122-5p	13,367.43	2.21	<0.001
	hsa-miR-4497	272.39	2.05	0.07
Cytoadhesion data				
Platelet-mediated agglutination, n = 50 vs. 19 UM				
	hsa-miR-3158-3p	1,180.96	−2.26	<0.001
	hsa-miR-320a	22,005.69	−1.48	0.001
	hsa-miR-4492	18.33	2.78	0.002
	hsa-miR-1290	1,011.34	−1.38	0.014
	hsa-miR-320b	1,191.44	−1.23	0.014
	hsa-miR-320c	408.32	−1.29	0.014
	hsa-miR-1246	3,907.45	−1.32	0.019
	hsa-miR-6741-5p	48.11	−1.81	0.023
	hsa-miR-1228-5p	82.73	−1.88	0.023
	hsa-miR-3195	16.35	2.21	0.023
	hsa-miR-7706	334.86	−1.00	0.023
gC1qR, n = 35 vs. 34 UM				
	hsa-miR-1-3p	622.35	2.09	0.003

*Positive fold change indicates overexpression in severe malaria and symptoms of severity compared to UM as well as parasites showing cytoadhesion compared to none. Total number of miRNAs in RNA sequencing data was 1,450. p value adjusted for multiple testing by the Benjamini-Hochberg method. baseMean, mean normalized expression of the miRNAs in all the samples; miRNA, microRNA; SA, severe anemia, SM, severe malaria; UM, uncomplicated malaria.

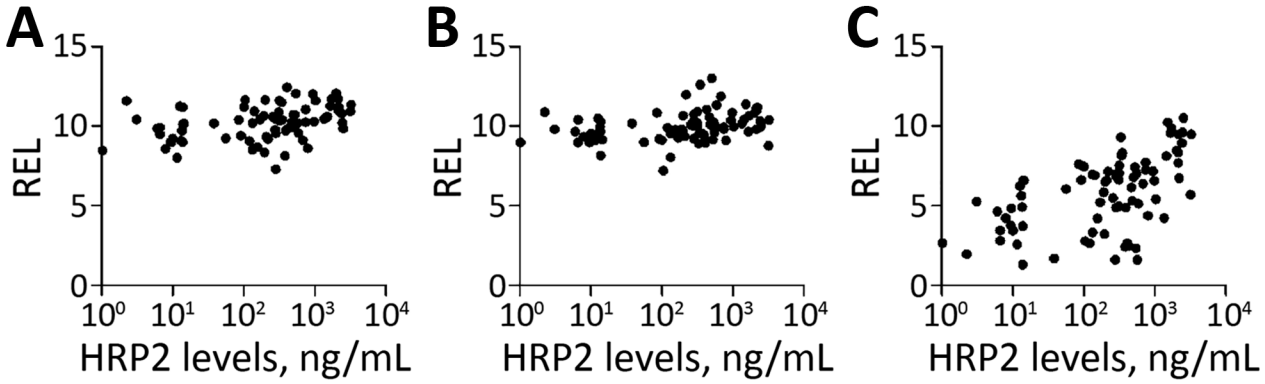

Figure 3. Spearman correlations between HRP2 levels and relative expression levels (RELs) of 3 miRNA in plasma samples from children with malaria, 2006, Mozambique. A) hsa-miR-10b-5p; B) hsa-miR-378a-3p; C) hsa-miR-4497. HRP2 levels and miRNA RELs were log transformed. The correlation analysis was adjusted for multiple testing by the Benjamini-Hochberg method. HRP2, histidine-rich protein 2; miRNA, microRNA; REL, relative expression levels.

Moreover, the detection of miRNAs associated with organ damage in host biofluids may provide an alternative to postmortem autopsies for determining the presence of parasites in host vital organs. This approach creates new opportunities to develop malaria diagnostic tools that can guide treatment decisions, and to understand the role of human miRNAs in several disease conditions (*23*).

In the discovery phase, 89 miRNAs were found to be differentially expressed in the media of HBE cells after incubation with an ePCR-cytoadherent *P. falciparum* strain compared with noncytoadherent parasites and noninfected erythrocytes. In addition, 15 miRNAs in plasma samples obtained from children were associated with SM, with specific severity symptoms, and with the cytoadherent *P. falciparum*

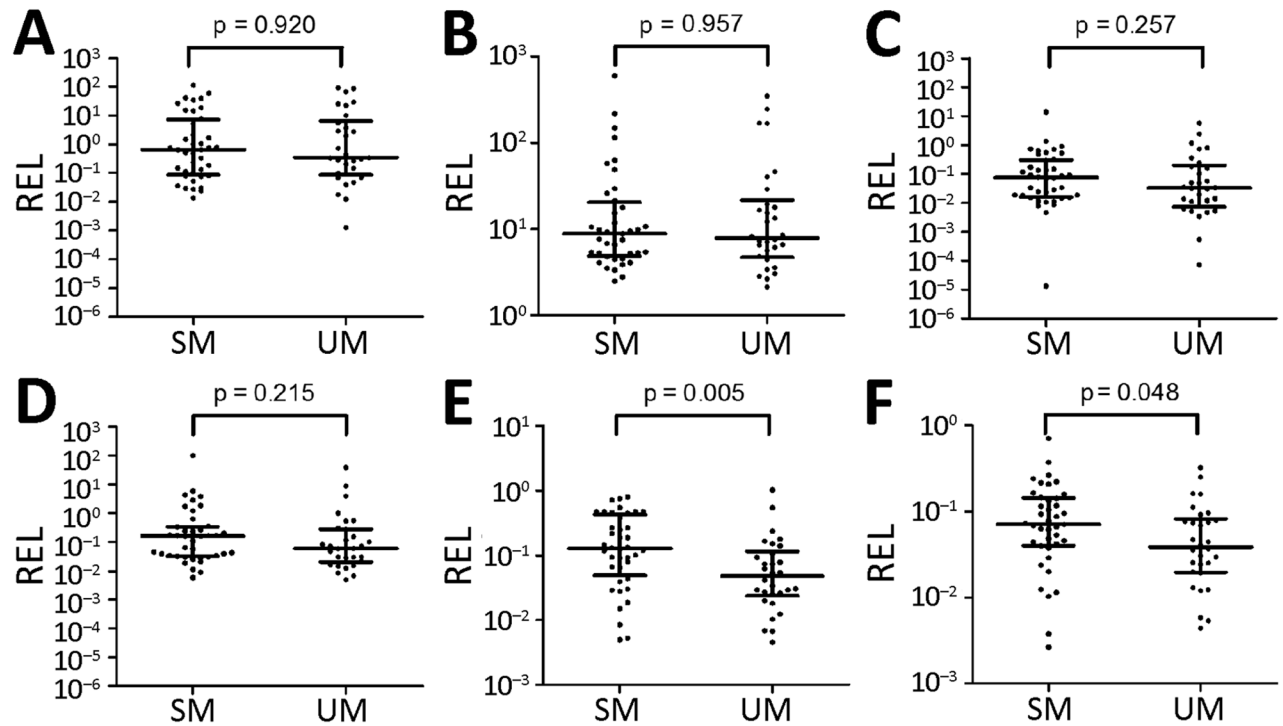

Figure 4. MiRNA validation in plasma samples of children with malaria, 2014, Mozambique. A) hsa-miR-122-5p; B) hsa-miR-320a; C) hsa-miR-1246; D) hsa-miR-1290; E) hsa-miR-3158-3p; F) hsa-miR-4497. RELs were calculated with respect to the mean of 2 endogenous controls (hsa-miR-30d-5p and hsa-miR-191–5p) and compared between children with SM and UM. Statistical differences were obtained by using the Mann-Whitney U test. Error bars represent medians and interquartile ranges. HRP2, histidine-rich protein 2; miRNA, microRNA; REL, relative expression levels; SM, severe malaria; UM, uncomplicated malaria.

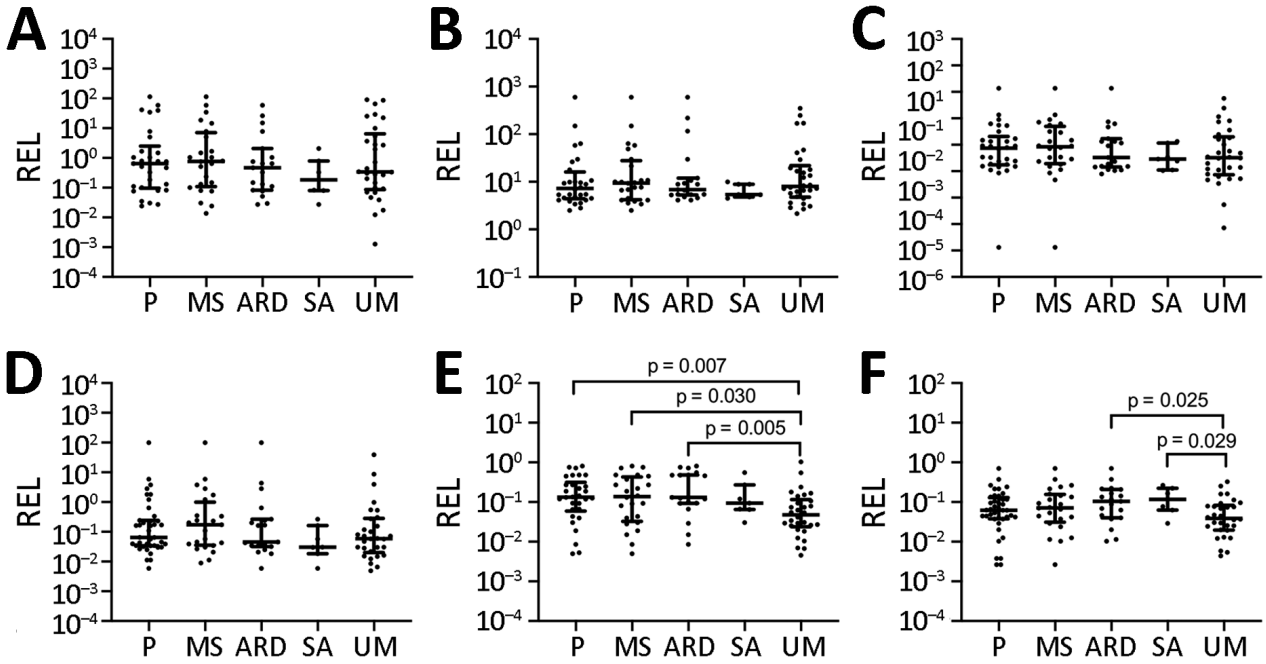

Figure 5. Association of microRNA levels with symptoms of severity in children with malaria, Mozambique, 2014. A) hsa-miR-122-5p; B) hsa-miR-320a; C) hsa-miR-1246; D) hsa-miR-1290; E) hsa-miR-3158-3p; F) hsa-miR-4497. RELs were calculated with respect to the mean of 2 endogenous controls (hsa-miR-30d-5p and hsa-miR-191–5p) and compared between children with UM and symptoms of severity. Distributions were compared using Mann-Whitney U test. Error bars represent medians and interquartile ranges. p values are shown for significant comparisons. ARD, acidosis or acute respiratory distress; MS, multiple seizures; P, prostration; REL, relative expression levels; SA, severe anemia; UM, uncomplicated malaria.

phenotype, compared with UM and noncytoadherent parasites. In the validation phase, we confirmed the higher abundance of hsa-miR-3158–3p and hsa-miR-4497 in children with SM than in children with UM. Prostration, multiple seizures, SA, and ARD symptoms of severity were associated with higher levels of hsa-miR-3158–3p and hsa-miR-4497. hsa-miR-4497 levels were also positively correlated with the parasite biomass as quantified by the levels of HRP2 in both the discovery and validation phases. Overall, these findings suggest that different physiopathological processes in SM and UM lead to differential expression of miRNAs in plasma.

HBE cells released a high number of the miRNAs when they were stimulated with an ePCR binding *P. falciparum* strain within the first hour of incubation. After 24 hours, the system stabilized; 1 miRNA (hsa-miR-451a) was found at higher levels in cell-conditioned media of HBE cells incubated with an ePCR binding strain than in cells stimulated with nonadherent (3D7-iE) or noninfected erythrocytes. miR-451 has been implicated in translocation to form a chimera with *Plasmodium* mRNAs to block their translation (*34*) and was also found to be abundant in sickle erythrocytes (*35*). In addition, it has been shown that parasites could reduce miR-451 levels in host fluids (*36*). However, this finding was not confirmed in plasmas from the children in this study. Five miRNA levels were higher in children with SM and severity symptoms (prostration, SA, and ARD) than in children with UM. *P. falciparum* cytoadhesion phenotypes (PM-agglutination and cytoadhesion to gC1qR) were also associated with the differential expression of miRNAs, suggesting that the interaction between PfEMP1 and host receptors leads to the secretion to plasma of specific miRNAs. Moreover, 3 miRNAs (hsa-miR-10b-5p, hsa-miR-378a-3p, and hsa-miR-4497) were positively correlated with HRP2 levels.

We selected 6 candidate miRNAs identified in the discovery phase to determine the validity of the previous results in an independent cohort of children in Mozambique. The relative expression of hsa-miR-3158–3p and hsa-miR-4497 was significantly higher in children with SM than in those with UM; hsa-miR-3158–3p levels were higher in children with prostration, multiple seizures, and ARD, and hsa-miR-4497 in children with SA and ARD. To our knowledge, hsa-miR-3158–3p, which is widely expressed in skin, spleen, kidney, and brain tissues (*37*), has been associated with bipolar disorders (*38*) but not with

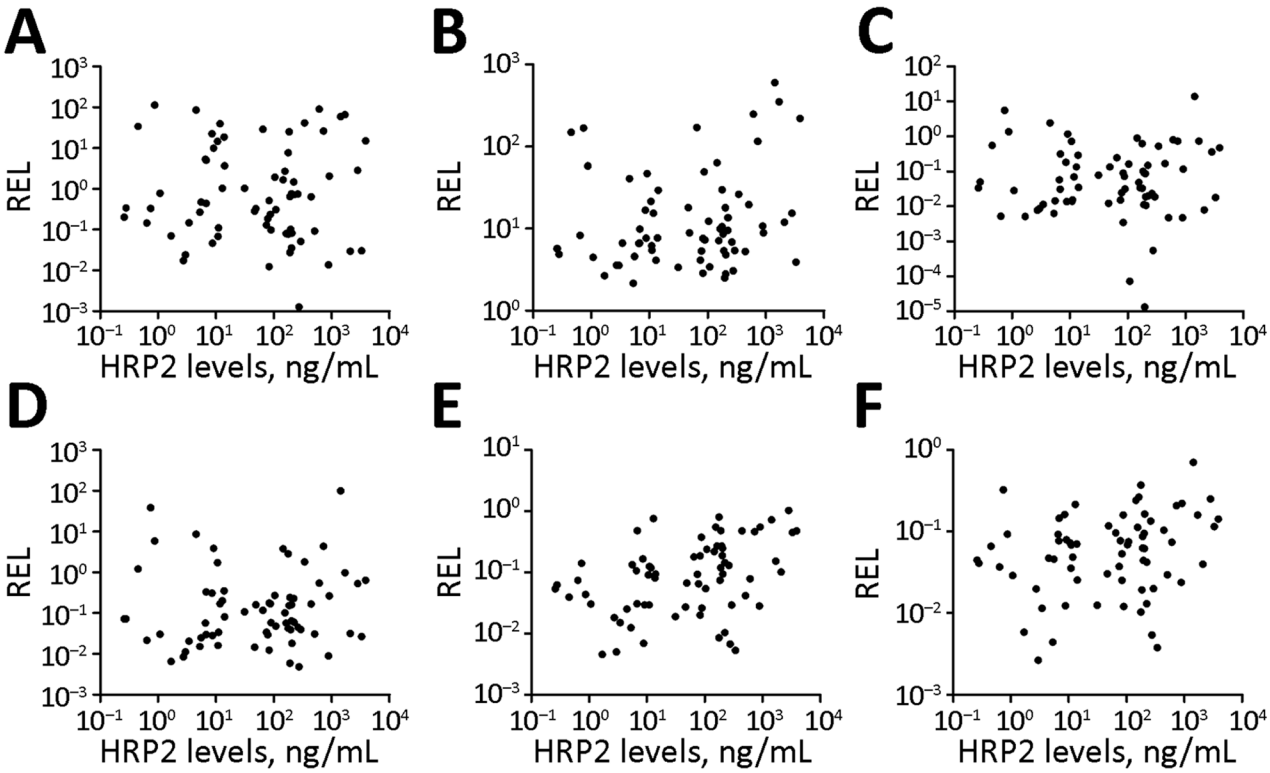

Figure 6. Spearman correlations between HRP2 levels and microRNA RELs in plasma samples from children with malaria, Mozambique, 2014. A) hsa-miR-122-5p; B) hsa-miR-320a; C) hsa-miR-1246; D) hsa-miR-1290; E) hsa-miR-3158-3p; F) hsa-miR-4497. HRP2 levels and microRNA RELs were log transformed. HRP2, histidine-rich protein 2; REL, relative expression levels.

other infectious diseases. Further validation is required for hsa-miR-3158–3p because the levels of this miRNA were found to be downregulated in the plasma from children recruited in 2006 with positive PM-agglutination compared with no PM-agglutination, a *P. falciparum* cytoadhesion phenotype which has been associated with malaria severity (*39*). However, the positive correlation of hsa-miR-4497 with HRP2 levels, which was consistently observed in the cohorts of children from 2006 and 2014, suggested that increasing parasite biomass associated with parasite sequestration may lead to higher levels of secretion of this specific miRNA by damaged tissues. The miRNA hsa-miR-4497 is widely expressed in the lymph nodes and spleen, kidney, and liver tissues (*37*). Overall, this study shows that hsa-miR-4497, which is also associated with SM, might be an interesting proxy marker of malaria severity. However, hsa-miR-4497 has been identified as a tumor suppressor (*40*) and associated with *Mycobacterium tuberculosis* infection (*41*). Therefore, longitudinal studies are required to assess the prognostic value of this miRNA, as well as to estimate its differential expression in children with severity due to nonmalarial infections.

Few of the most expressed miRNAs found in our study, which represent 70% of the total miRNA counts in plasma samples, have been previously reported as highly abundant in plasma samples (*28,42*). According to public data deposited in the miRmine database (*43*), hsa-miR-486–5p and hsa-miR-451a are the 2 most abundant miRNAs in plasma; both were among the 10 most expressed miRNAs in our study. Although no data are available on miRNAs from cell-conditioned media of HBE cells, miRNA data from other cell types, such as primary tissue explants, primary stromal cells, and breast cancer cell lines, also show low miRNA yield (*44*), similar to this study. Our observation indicates that RNA sequencing data obtained in this study is of good quality and can be used for posterior analysis with high confidence.

The first limitation of our study is that we used only HBE cells and ePCR binding parasites for the in vitro assay and therefore may have missed miRNAs produced by other parasite-host interactions contributing to SM. Second, plasma samples used in this study were collected retrospectively. Therefore, factors before small RNA sequencing and TaqMan-qRT-PCR, such as time taken between centrifugation,

storage, and storage temperature, might have varied among the samples, affecting miRNA plasma levels (*45,46*). However, confirmation of findings in both the study cohorts suggest a minimal effect of preanalysis conditions in the results. Third, variations in the number of miRNAs identified in replicates of in vitro experiments may have led to the loss of some miRNAs. Fourth, the lack of tissue samples from organs with *P. falciparum* sequestration restricted the histological confirmation of identified miRNAs, and the presence of co-infections other than blood culture positive bacteremia cannot be neglected in the studied plasma samples. Finally, the association of each miRNA with specific symptoms that are part of the SM case definition may need further validation using a larger sample size, considering that our numbers were relatively small for individual SM criteria. In addition, future studies using machine-learning approaches would enable the identification of a combination of miRNAs that may detect SM pathologies.

In conclusion, the profiling of miRNAs in media from HBE cells after incubation with a cytoadherent *P. falciparum* strain and in plasma from children with different clinical manifestations enabled us to identify promising miRNA candidates for characterizing severe malaria, specifically hsa-miR-4497. This study is a base for future analyses to understand the value of these miRNAs as a prognostic biomarker and for disentangling the etiology of SM.

Acknowledgments

We thank the children who participated in the study; the staff of the Manhiça District Hospital; the clinical officers, field supervisors, and data managers; G. Cabrera, L. Mussacate, N. Ernesto José, and A. Nhabomba for their contribution to the collection of parasites; and L. Puyol for her laboratory management, as well as everyone who supported this study directly or indirectly. We also thank Ruhi Sikka, Varun Sharma, Rebecca Smith-Aguasca, Malia Skjefte, and Catriona Patterson for their useful comments on this manuscript.

This work was supported by the Instituto de Salud Carlos III (PI13/01478 cofunded by the Fondo Europeo de Desarrollo Regional [FEDER], grant no. CES10/021-I3SNS to A.M. and no. CP11/00269 from the Miguel Servet program to Q.B.). H.G. was supported by the Science and Engineering Research Board (SERB), Department of Science & Technology, Government of India (Overseas Postdoctoral Fellowship, SB/OS/PDF043/201516), January 2017–January 2019. ISGlobal is a member of the CERCA Programme, Generalitat de Catalunya (http://cerca.cat/en/suma). CISM is supported by the Government of Mozambique and the Spanish Agency for International Development (AECID). This research is part of ISGlobal's Program on the Molecular Mechanisms of Malaria, which is partially supported by the Fundación Ramón Areces.

H.G. and M.R. carried out the molecular analysis and results interpretation and wrote the first draft of this manuscript. P.C. also carried out molecular analysis and conducted cytoadhesion assays. A.S., R.V., L.M., and I.C. participated in fieldwork; collected clinical and epidemiological data, plasma samples, and dried blood drop filter papers; and performed microscopy. A.J., X.M.V., and D.B. participated in HRP2 analysis. M.R., P.C., H.G., L.P., A.B., and M.B. participated in bioinformatics and statistical analyses. Q.B. and A.M. participated in the study design, supervision, funding acquisition, project administration and coordinated all the stages of the project. All authors reviewed and approved the final manuscript. The datasets analyzed in this study are available from the corresponding author on request.

About the Author

Dr. Gupta is a molecular biologist and an early career malaria disease researcher. His research focuses on host and parasite factors associated with severe malaria, and on the use of molecular tools for the active surveillance of emerging drug resistance, gene deletions, and afebrile malaria in malaria-endemic regions.

References

1. Dondorp AM, Fanello CI, Hendriksen IC, Gomes E, Seni A, Chhaganlal KD, et al.; AQUAMAT group. Artesunate versus quinine in the treatment of severe falciparum malaria in African children (AQUAMAT): an open-label, randomised trial. Lancet. 2010;376:1647–57. https://doi.org/10.1016/S0140-6736(10)61924-1
2. Gravenor MB, van Hensbroek MB, Kwiatkowski D. Estimating sequestered parasite population dynamics in cerebral malaria. Proc Natl Acad Sci U S A. 1998;95:7620–4. https://doi.org/10.1073/pnas.95.13.7620
3. Miller LH, Baruch DI, Marsh K, Doumbo OK. The pathogenic basis of malaria. Nature. 2002;415:673–9. https://doi.org/10.1038/415673a
4. Dorovini-Zis K, Schmidt K, Huynh H, Fu W, Whitten RO, Milner D, et al. The neuropathology of fatal cerebral malaria in Malawian children. Am J Pathol. 2011;178:2146–58. https://doi.org/10.1016/j.ajpath.2011.01.016
5. Nagatake T, Hoang VT, Tegoshi T, Rabbege J, Ann TK, Aikawa M. Pathology of falciparum malaria in Vietnam. Am J Trop Med Hyg. 1992;47:259–64. https://doi.org/10.4269/ajtmh.1992.47.259
6. Milner DA Jr, Whitten RO, Kamiza S, Carr R, Liomba G, Dzamalala C, et al. The systemic pathology of cerebral malaria in African children. Front Cell Infect Microbiol. 2014;4:104. https://doi.org/10.3389/fcimb.2014.00104
7. White NJ, Turner GD, Day NP, Dondorp AM. Lethal malaria: Marchiafava and Bignami were right. J Infect Dis. 2013;208:192–8. https://doi.org/10.1093/infdis/jit116

8. Rowe JA, Claessens A, Corrigan RA, Arman M. Adhesion of *Plasmodium falciparum*-infected erythrocytes to human cells: molecular mechanisms and therapeutic implications. Expert Rev Mol Med. 2009;11:e16. https://doi.org/10.1017/S1462399409001082
9. Turner L, Lavstsen T, Berger SS, Wang CW, Petersen JE, Avril M, et al. Severe malaria is associated with parasite binding to endothelial protein C receptor. Nature. 2013;498:502–5. https://doi.org/10.1038/nature12216
10. Jensen AR, Adams Y, Hviid L. Cerebral *Plasmodium falciparum* malaria: The role of PfEMP1 in its pathogenesis and immunity, and PfEMP1-based vaccines to prevent it. Immunol Rev. 2020;293:230–52. https://doi.org/10.1111/imr.12807
11. Sahu PK, Satpathi S, Behera PK, Mishra SK, Mohanty S, Wassmer SC. Pathogenesis of cerebral malaria: new diagnostic tools, biomarkers, and therapeutic approaches. Front Cell Infect Microbiol. 2015;5:75. https://doi.org/10.3389/fcimb.2015.00075
12. Erdman LK, Petes C, Lu Z, Dhabangi A, Musoke C, Cserti-Gazdewich CM, et al. Chitinase 3-like 1 is induced by *Plasmodium falciparum* malaria and predicts outcome of cerebral malaria and severe malarial anaemia in a case–control study of African children. Malar J. 2014;13:279. https://doi.org/10.1186/1475-2875-13-279
13. Lucchi NW, Jain V, Wilson NO, Singh N, Udhayakumar V, Stiles JK. Potential serological biomarkers of cerebral malaria. Dis Markers. 2011;31:327–35. https://doi.org/10.1155/2011/345706
14. Tahar R, Albergaria C, Zeghidour N, Ngane VF, Basco LK, Roussilhon C. Plasma levels of eight different mediators and their potential as biomarkers of various clinical malaria conditions in African children. Malar J. 2016;15:337. https://doi.org/10.1186/s12936-016-1378-3
15. Dondorp AM, Desakorn V, Pongtavornpinyo W, Sahassananda D, Silamut K, Chotivanich K, et al. Estimation of the total parasite biomass in acute falciparum malaria from plasma PfHRP2. PLoS Med. 2005;2:e204. https://doi.org/10.1371/journal.pmed.0020204
16. Hendriksen IC, Mwanga-Amumpaire J, von Seidlein L, Mtove G, White LJ, Olaosebikan R, et al. Diagnosing severe falciparum malaria in parasitemic African children: a prospective evaluation of plasma PfHRP2 measurement. PLoS Med. 2012;9:e1001297. https://doi.org/10.1371/journal.pmed.1001297
17. Cortez MA, Bueso-Ramos C, Ferdin J, Lopez-Berestein G, Sood AK, Calin GA. MicroRNAs in body fluids—the mix of hormones and biomarkers. Nat Rev Clin Oncol. 2011;8:467–77. https://doi.org/10.1038/nrclinonc.2011.76
18. Mitchell PS, Parkin RK, Kroh EM, Fritz BR, Wyman SK, Pogosova-Agadjanyan EL, et al. Circulating microRNAs as stable blood-based markers for cancer detection. Proc Natl Acad Sci U S A. 2008;105:10513–8. https://doi.org/10.1073/pnas.0804549105
19. Hakimi MA, Cannella D. Apicomplexan parasites and subversion of the host cell microRNA pathway. Trends Parasitol. 2011;27:481–6. https://doi.org/10.1016/j.pt.2011.07.001
20. El-Assaad F, Hempel C, Combes V, Mitchell AJ, Ball HJ, Kurtzhals JA, et al. Differential microRNA expression in experimental cerebral and noncerebral malaria. Infect Immun. 2011;79:2379–84. https://doi.org/10.1128/IAI.01136-10
21. Baro B, Deroost K, Raiol T, Brito M, Almeida AC, de Menezes-Neto A, et al. *Plasmodium vivax* gametocytes in the bone marrow of an acute malaria patient and changes in the erythroid miRNA profile. PLoS Negl Trop Dis. 2017;11:e0005365. https://doi.org/10.1371/journal.pntd.0005365
22. Xue X, Zhang Q, Huang Y, Feng L, Pan W. No miRNA were found in *Plasmodium* and the ones identified in erythrocytes could not be correlated with infection. Malar J. 2008;7:47. https://doi.org/10.1186/1475-2875-7-47
23. Rubio M, Bassat Q, Estivill X, Mayor A. Tying malaria and microRNAs: from the biology to future diagnostic perspectives. Malar J. 2016;15:167. https://doi.org/10.1186/s12936-016-1222-9
24. StatsTutor. Spearman's correlation. 2011 [cited 2020 Nov 23]. http://www.statstutor.ac.uk/resources/uploaded/spearmans.pdf
25. Mayor A, Serra-Casas E, Bardají A, Sanz S, Puyol L, Cisteró P, et al. Sub-microscopic infections and long-term recrudescence of *Plasmodium falciparum* in Mozambican pregnant women. Malar J. 2009;8:9. https://doi.org/10.1186/1475-2875-8-9
26. Taylor SM, Mayor A, Mombo-Ngoma G, Kenguele HM, Ouédraogo S, Ndam NT, et al. A quality control program within a clinical trial consortium for PCR protocols to detect *Plasmodium* species. J Clin Microbiol. 2014;52:2144–9. https://doi.org/10.1128/JCM.00565-14
27. Wang J, Chen J, Chang P, LeBlanc A, Li D, Abbruzzesse JL, et al. MicroRNAs in plasma of pancreatic ductal adenocarcinoma patients as novel blood-based biomarkers of disease. Cancer Prev Res (Phila). 2009;2:807–13. https://doi.org/10.1158/1940-6207.CAPR-09-0094
28. Rubio M, Bustamante M, Hernandez-Ferrer C, Fernandez-Orth D, Pantano L, Sarria Y, et al. Circulating miRNAs, isomiRs, and small RNA clusters in human plasma and breast milk. PLoS One. 2018;13:e0193527. https://doi.org/10.1371/journal.pone.0193527
29. Pantano L, Estivill X, Martí E. SeqBuster, a bioinformatic tool for the processing and analysis of small RNAs datasets, reveals ubiquitous miRNA modifications in human embryonic cells. Nucleic Acids Res. 2010;38:e34. https://doi.org/10.1093/nar/gkp1127
30. Love MI, Huber W, Anders S. Moderated estimation of fold change and dispersion for RNA-seq data with DESeq2. Genome Biol. 2014;15:550. https://doi.org/10.1186/s13059-014-0550-8
31. Marabita F, de Candia P, Torri A, Tegnér J, Abrignani S, Rossi RL. Normalization of circulating microRNA expression data obtained by quantitative real-time RT-PCR. Brief Bioinform. 2016;17:204–12. https://doi.org/10.1093/bib/bbv056
32. Pantano L, Estivill X, Martí E. A non-biased framework for the annotation and classification of the non-miRNA small RNA transcriptome. Bioinformatics. 2011;27:3202–3. https://doi.org/10.1093/bioinformatics/btr527
33. Kirschner MB, Edelman JJ, Kao SC, Vallely MP, van Zandwijk N, Reid G. The impact of hemolysis on cell-free microRNA biomarkers. Front Genet. 2013;4:94. https://doi.org/10.3389/fgene.2013.00094
34. LaMonte G, Philip N, Reardon J, Lacsina JR, Majoros W, Chapman L, et al. Translocation of sickle cell erythrocyte microRNAs into *Plasmodium falciparum* inhibits parasite translation and contributes to malaria resistance. Cell Host Microbe. 2012;12:187–99. https://doi.org/10.1016/j.chom.2012.06.007
35. Chen SY, Wang Y, Telen MJ, Chi JT. The genomic analysis of erythrocyte microRNA expression in sickle cell diseases. PLoS One. 2008;3:e2360. https://doi.org/10.1371/journal.pone.0002360
36. Rathjen T, Nicol C, McConkey G, Dalmay T. Analysis of short RNAs in the malaria parasite and its red blood cell host. FEBS Lett. 2006;580:5185–8. https://doi.org/10.1016/j.febslet.2006.08.063

37. Ludwig N, Leidinger P, Becker K, Backes C, Fehlmann T, Pallasch C, et al. Distribution of miRNA expression across human tissues. Nucleic Acids Res. 2016;44:3865–77. https://doi.org/10.1093/nar/gkw116
38. Maffioletti E, Cattaneo A, Rosso G, Maina G, Maj C, Gennarelli M, et al. Peripheral whole blood microRNA alterations in major depression and bipolar disorder. J Affect Disord. 2016;200:250–8. https://doi.org/10.1016/j.jad.2016.04.021
39. Mayor A, Hafiz A, Bassat Q, Rovira-Vallbona E, Sanz S, Machevo S, et al. Association of severe malaria outcomes with platelet-mediated clumping and adhesion to a novel host receptor. PLoS One. 2011;6:e19422. https://doi.org/10.1371/journal.pone.0019422
40. Chen X, Zhang L, Tang S. MicroRNA-4497 functions as a tumor suppressor in laryngeal squamous cell carcinoma via negatively modulation the GBX2. Auris Nasus Larynx. 2019;46:106–13. https://doi.org/10.1016/j.anl.2018.05.005
41. Das K, Saikolappan S, Dhandayuthapani S. Differential expression of miRNAs by macrophages infected with virulent and avirulent *Mycobacterium tuberculosis*. Tuberculosis (Edinb). 2013;93(Suppl):S47–50. https://doi.org/10.1016/S1472-9792(13)70010-6
42. Tonge DP, Gant TW. What is normal? Next generation sequencing-driven analysis of the human circulating miRNAOme. BMC Mol Biol. 2016;17:4. https://doi.org/10.1186/s12867-016-0057-9
43. Panwar B, Omenn GS, Guan Y. miRmine: a database of human miRNA expression profiles. Bioinformatics. 2017;33:1554–60. https://doi.org/10.1093/bioinformatics/btx019
44. Glynn CL, Khan S, Kerin MJ, Dwyer RM. Isolation of secreted microRNAs (miRNAs) from cell-conditioned media. MicroRNA. 2013;2:14–9. https://doi.org/10.2174/2211536611302010003
45. Glinge C, Clauss S, Boddum K, Jabbari R, Jabbari J, Risgaard B, et al. Stability of circulating blood-based microRNAs—pre-analytic methodological considerations. PLoS One. 2017;12:e0167969. https://doi.org/10.1371/journal.pone.0167969
46. Sourvinou IS, Markou A, Lianidou ES. Quantification of circulating miRNAs in plasma: effect of preanalytical and analytical parameters on their isolation and stability. J Mol Diagn. 2013;15:827–34. https://doi.org/10.1016/j.jmoldx.2013.07.005

Address for correspondence: Himanshu Gupta, ISGlobal, Hospital Clínic, Universitat de Barcelona, Carrer Rosselló 153 (CEK Bldg), E-08036 Barcelona, Spain; email: himanshu.gupta@isglobal.org or himanshugupta.hcu@gmail.com

Article DOI: https://doi.org/10.3201/eid2702.191795

Plasma MicroRNA Profiling of *Plasmodium falciparum* Biomass and Association with Severity of Malaria Disease

Appendix

Material and Methods

Study Population

Clinical malaria was defined as the presence of fever (axillary temperature ≥37.5°C) with an asexual parasitemia of *Pf* ≥500/µL. Children with severe malaria (SM) were those with ≥1 of the following symptoms: cerebral malaria (Blantyre Coma Score ≤2), severe anemia (SA; packed cell volume <15% or hemoglobin <5 g/dL), acidosis or acute respiratory distress (ARD; lactate >5 mM and/or chest indrawing or deep breathing), prostration (inability to sit or breastfeed in children old enough to do so based on their age), hypoglycemia (blood glucose <2.2 mM), and multiple seizures (≥2 convulsions in the preceding 24 h) following the modified World Health Organization criteria (*1*). Children with uncomplicated malaria (UM) were those with clinical malaria but not manifesting any signs or symptoms of severity mentioned above (*2*). The presence of concomitant bacteremia was tested in all SM cases using blood cultures; and children with positive bacteremia were excluded. Children with SM were treated according to Mozambican national guidelines with parenteral quinine in 2006 or parenteral artesunate (complemented with an oral artemisinin-based combination therapy) in 2014, and those with UM were treated with a combination of oral amodiaquine and sulfadoxine−pyrimethamine (Fansidar; Roche Pharma (Schweiz) AG, https://www.roche.ch/pharma.htm) in 2006 or with artemether-lumefantrine (Coartem; Novartis, https://www.novartis.com) in 2014. We collected 10 mL of heparinized blood from study participants and processed within 2 hours after collection. Filter paper dried blood spots of 60µL blood were prepared from the vacutainer blood. After centrifugation at 1,000 rpm for 10 min at 4°C, plasma was stored at −20°C. The 2014 study was conducted as a quasi-exact repetition of the 2006 study; the only difference was that cases and

controls were matched by parasitemia level. We assessed biochemistry parameters (glucose and lactate) using Vitros DT60-II (Ortho Clinical Diagnostics, https://www.orthoclinicaldiagnostics.com and a full blood count using Sysmex Kx21 analyzers (Sysmex, https://www.sysmex.co.jp) for each patient.

Parasitological Determinations

Histidine-rich protein 2 (HRP2) levels were quantified using commercially available enzyme-linked immunosorbent assay kits (Malaria Ag CELISA; Cellabs Pty. Ltd, https://www.cellabs.com.au) and an in-house highly sensitive quantitative bead suspension array based on Luminex technology. In brief, plasma samples were incubated overnight at 4°C with 2,000 magnetic beads to a final dilution of 1:10. After washing, beads were sequentially incubated with 100 µL of in-house biotinylated antibody α-HRP2 (MBS832975, MyBiSource, https://www.mybiosource.com) at 1 µg/mL and with streptavidin-PE (42250–1ML, Sigma Aldrich, https://www.sigmaaldrich.com) at 1:1000 dilution. Finally, beads were washed and resuspended in assay buffer, and the plate was read using the Luminex xMAP 100/200 analyzer (Luminex Corp., https://www.luminexcorp.com). A minimum of 50 microspheres/analyte were acquired and results were exported as crude median fluorescent intensity (MFI). Background (blank) MFIs were subtracted and normalized to account for plate-to-plate variation. Quantification was performed against a 5-parameter logistic regression curve fitted from a calibration curve consisting of recombinant protein HRP2 type A (890015, Microcoat GmbH, https://www.microcoat.de).

Pf Cytoadhesion Assays

Human brain microvascular endothelial cells (reference no. P10361 Innoprot, https://innoprot.com) were cultured in 12-well plates following the supplier's recommendations and were left until 40% confluency was achieved. HBE cells were incubated in triplicate with *Pf*-iEs at trophozoite stage of the ePCR binding FCR3 strain (ePCR-iE, which expresses the PfEPM1 protein that binds to ePCR receptor) and 3D7 strain (3D7-iE, a strain without the protein that binds to ePCR receptor) with 5% of both parasitemia and hematocrit. Noninfected erythrocytes were used as negative control. The cell-conditioned media of each group were collected after 1 h (t1) and 24 h of stimulation (t24). Next day, HBE cells were stimulated as described above, after 1-hour incubation in agitation, cells were washed $\geq$10 times with binding media and fixed with 2% glutaraldehyde (Sigma) in PBS (Gibco, Thermo Fisher) overnight to

assess adhesion by light microscopy. After washing with water, cells were stained with 10% Giemsa. iE and niE bound were counted in 6 different wells/assay in ≥500 nuclei cell/well. Results were presented as the number of adhered iE per 500 nuclei of cells. Estimation of *Pf* adhesion to purified receptors (CD36, CD54, and g1CqR) as well as platelet-mediated (PM)-agglutination and rosetting was performed as described elsewhere (*2*,*3*). Cytoadherence was defined as positive only if the number of iEs bound per mm^2 > the mean binding +2 SD to Duffy-Fc coated petri dishes. *Pf* isolates were considered positive for PM clumping if the frequency of clumps was higher in the presence of platelets than in buffer-control and for rosetting if the frequency of rosettes was >2% (*2*,*4*).

Small RNA Sequencing

Before RNA extraction, the level of hemolysis in plasma samples was assessed by spectrophotometry (EPOCH, BioTek) at a wavelength of 414nm (absorbance peak of free hemoglobin). Samples were classified as nonhemolysed if the optical density at 414nm <0.2 (*5*). RNA was extracted from cell-conditioned media (3 mL) using the miRNeasy tissues/cells kit and plasma samples (1 mL) using miRNeasy plasma/serum kit (both QIAGEN, https://www.qiagen.com), with the use of 5µg UltraPure glycogen/sample (Invitrogen, Thermo Fisher). Given that the plasma samples were conserved in heparin, RNA was precipitated with lithium chloride (LiCl) as described elsewhere (*6*). Purified RNA quality and quantity were determined using the Bioanalyzer (Agilent Technologies, https://www.agilent.com) followed by preparation of libraries using NEBNext Small RNA Library Prep Set for Illumina (New England Biolabs, https://www.neb.com), then separation of libraries in polyacrylamide gels (Novex; Invitrogen). The Bioanalyzer was again used to quantify and assess the size of the libraries. Further, libraries were pooled at the same equimolar concentrations and no more than 18 libraries were sequenced in the same lane using a HiSeq 2000 (Illumina) platform following the protocol for small RNAs (*7*).

A previously published pipeline was used to assess the sequencing quality, identification, and quantification of small RNAs and normalization (*7*). First, a quality control (QC) was conducted using FASTX-Toolkit and FastQ Screen. After adaptor removing, reads with the following features were removed: reads <18 nt; mean PHRED scores <30; and low complexity reads based on the mean score of the read. Good quality reads were then annotated to main RNA categories (tRNA, rRNA, and miRNAs), and miRNA complexity was estimated as the number of

distinct miRNAs observed in each sample. Finally, contamination with RNA from other species was evaluated by mapping reads to clade-specific mature miRNA sequences extracted from miRBase v21 (*8*). The tested species categories include animal sponges, nematodes, insects, lophotrochozoan, echinoderms, fish, birds, reptiles, rodents, and primates.

Sequences that passed the QC were subjected to the seqBuster/seqCluster tool that retrieves miRNA and isomiRs counts (*9,10*). To detect miRNAs and isomiRs, reads were mapped to the precursors and annotated to miRNAs or isomiRs using miRBase version 21 with the miraligner (*9*). DESeq2 R package v.1.10.1 (R version 3.3.2) (*11*) was used to perform an internal normalization in which the counts for a miRNA in each sample were divided by the median of the ratios of observed counts to the geometric mean of each corresponding miRNAs over all samples.

Reverse Transcription Quantitative PCR

We used 50 µL of plasma with no hemolysis from the children recruited in 2014 for RNA extraction as described above. A synthetic RNA mimicking ath-miR-159a (*Arabidopsis thaliana*; Metabion, http://www.metabion.com) was added after lysis reaction at a final concentration of 1.5 pM. cDNA synthesis and RT-qPCR (ABI PRISM 7500 HT Real-Time System; Applied Biosystems) were performed using the TaqMan Advanced miRNA assays. A standard curve of 5 serially diluted points was prepared with cDNA of 6 randomly selected samples and run in triplicate for each miRNA. Results were normalized using a combination of endogenous controls (ECs). The selection of ECs was based on the following criteria: a) reported in scientific literature as previously used as ECs (*12,13*), b) coefficient of variance (CV) of normalized counts across all samples $\leq$5%, c) basemean $\geq$3000, d) SD $\leq$1, and e) $\log_2$fold change between SM and UM patients $\leq$1. Finally, the best 2 ECs tested as housekeepings using the NormFinder (*14*) were used for normalization of RT-qPCR data. miRNA relative expression levels (RELs) were calculated with the $2^{-\Delta Ct}$ method, where ΔCt = [Ct (miRNA) – Mean Ct (ECs)], considering efficiencies of 100% for all the miRNAs and ECs (*12*).

In silico Analysis

The selected miRNAs were screened through 4 different gene target prediction programs: DIANA-microT-CDS (*15*), MiRDIP (*16*), MirGate (*17*), and TargetScan (http://www.targetscan.org/vert_71). Identified gene targets of each program were compared

using an online tool, Venny2.1.0 (http://bioinfogp.cnb.csic.es/tools/venny). The gene targets that occurred in more than one database were selected and screened through the miRTarBase (*18*) online program to check if these genes have been experimentally validated previously. These gene targets were anticipated to be true positive targets present at detectable levels in field samples. The identified gene targets were further analyzed by DAVID 6.8 using *Homo sapiens* as the reference species. Genes were clustered to Gene Ontology terms and KEGG pathways (fold enrichment >1.5, $p<0.05$).

Statistical Analysis

Differential expression of miRNAs and isomiRs was assessed using DESEq2 and IsomiRs packages in R (*9,10*), which use negative binomial generalized linear models adjusted for multiple testing with the false discovery rate (FDR) by the Benjamini-Hochberg method (*19*). Those with an FDR $\leq$5% were selected for posterior analysis. Analysis of the modification in the bases of the seed region was carried using isomiR package to determine a possible change in the target messenger RNAs. We performed Mann-Whitney U test to compare continuous data and χ^2 tests to compare categorical data. Spearman correlation analysis was performed to assess the correlation of miRNA RELs (log transformed) with log transformed HRP2 levels. A two-sided $p < 0.05$ was considered statistically significant. All statistical analyses were performed using R 3.3.2 in Linux-based system and graphs were prepared with GraphPad.

References

1. World Health Organization. Guidelines for the treatment of malaria. 3rd ed. 2015 [cited 2020 Aug 6]. https://www.who.int/malaria/publications/atoz/9789241549127

2. Mayor A, Hafiz A, Bassat Q, Rovira-Vallbona E, Sanz S, Machevo S, et al. Association of severe malaria outcomes with platelet-mediated clumping and adhesion to a novel host receptor. PLoS One. 2011;6:e19422. PubMed https://doi.org/10.1371/journal.pone.0019422

3. Roberts DJ, Craig AG, Berendt AR, Pinches R, Nash G, Marsh K, et al. Rapid switching to multiple antigenic and adhesive phenotypes in malaria. Nature. 1992;357:689–92. PubMed https://doi.org/10.1038/357689a0

4. Magallón-Tejada A, Machevo S, Cisteró P, Lavstsen T, Aide P, Rubio M, et al. Cytoadhesion to gC1qR through *Plasmodium falciparum* erythrocyte membrane protein 1 in severe malaria. PLoS Pathog. 2016;12:e1006011. PubMed https://doi.org/10.1371/journal.ppat.1006011

5. Kirschner MB, Edelman JJ, Kao SC, Vallely MP, van Zandwijk N, Reid G. The impact of hemolysis on cell-free microRNA biomarkers. Front Genet. 2013;4:94. PubMed https://doi.org/10.3389/fgene.2013.00094

6. Wang J, Chen J, Chang P, LeBlanc A, Li D, Abbruzzesse JL, et al. MicroRNAs in plasma of pancreatic ductal adenocarcinoma patients as novel blood-based biomarkers of disease. Cancer Prev Res (Phila). 2009;2:807–13. PubMed https://doi.org/10.1158/1940-6207.CAPR-09-0094

7. Rubio M, Bustamante M, Hernandez-Ferrer C, Fernandez-Orth D, Pantano L, Sarria Y, et al. Circulating miRNAs, isomiRs and small RNA clusters in human plasma and breast milk. PLoS One. 2018;13:e0193527. PubMed https://doi.org/10.1371/journal.pone.0193527

8. Griffiths-Jones S, Grocock RJ, van Dongen S, Bateman A, Enright AJ. miRBase: microRNA sequences, targets and gene nomenclature. Nucleic Acids Res. 2006;34:D140–4. PubMed https://doi.org/10.1093/nar/gkj112

9. Pantano L, Estivill X, Martí E. SeqBuster, a bioinformatic tool for the processing and analysis of small RNAs datasets, reveals ubiquitous miRNA modifications in human embryonic cells. Nucleic Acids Res. 2010;38:e34. PubMed https://doi.org/10.1093/nar/gkp1127

10. Pantano L, Estivill X, Martí E. A non-biased framework for the annotation and classification of the non-miRNA small RNA transcriptome. Bioinformatics. 2011;27:3202–3. PubMed https://doi.org/10.1093/bioinformatics/btr527

11. Love MI, Huber W, Anders S. Moderated estimation of fold change and dispersion for RNA-seq data with DESeq2. Genome Biol. 2014;15:550. PubMed https://doi.org/10.1186/s13059-014-0550-8

12. Marabita F, de Candia P, Torri A, Tegnér J, Abrignani S, Rossi RL. Normalization of circulating microRNA expression data obtained by quantitative real-time RT-PCR. Brief Bioinform. 2016;17:204–12. PubMed https://doi.org/10.1093/bib/bbv056

13. Yeri A, Courtright A, Reiman R, Carlson E, Beecroft T, Janss A, et al. Total extracellular small RNA profiles from plasma, saliva, and urine of healthy subjects. Sci Rep. 2017;7:44061. PubMed https://doi.org/10.1038/srep44061

14. Andersen CL, Jensen JL, Ørntoft TF. Normalization of real-time quantitative reverse transcription-PCR data: a model-based variance estimation approach to identify genes suited for normalization, applied to bladder and colon cancer data sets. Cancer Res. 2004;64:5245–50. PubMed https://doi.org/10.1158/0008-5472.CAN-04-0496

15. Paraskevopoulou MD, Georgakilas G, Kostoulas N, Vlachos IS, Vergoulis T, Reczko M, et al. DIANA-microT web server v5.0: service integration into miRNA functional analysis workflows. Nucleic Acids Research. 2013;41:W169–73.

16. Tokar T, Pastrello C, Rossos AEM, Abovsky M, Hauschild AC, Tsay M, et al. mirDIP 4.1-integrative database of human microRNA target predictions. Nucleic Acids Res. 2018;46(D1):D360–70. PubMed https://doi.org/10.1093/nar/gkx1144

17. Andrés-León E, González Peña D, Gómez-López G, Pisano DG. miRGate: a curated database of human, mouse and rat miRNA-mRNA targets. Database. 2015;2015:bav035.

18. Chou CH, Shrestha S, Yang CD, Chang NW, Lin YL, Liao KW, et al. miRTarBase update 2018: a resource for experimentally validated microRNA-target interactions. Nucleic Acids Res. 2018;46(D1):D296–302. PubMed https://doi.org/10.1093/nar/gkx1067

19. Benjamini Y, Drai D, Elmer G, Kafkafi N, Golani I. Controlling the false discovery rate in behavior genetics research. Behav Brain Res. 2001;125:279–84. PubMed https://doi.org/10.1016/S0166-4328(01)00297-2

Appendix Table 1. Characteristics of microRNAs detected in cell-conditioned media of human brain endothelial cells exposed to *Plasmodium falciparum*−infected and noninfected erythrocytes*

Sample	Total reads	Quality filtered	Complexity filtered	Length filtered	Good-quality reads	rRNA	tRNA	miRNA	Unknown	Different miRNAs
t1_niE-1	4,681,945	4	34	337,979	4,343,966	270,763	2,366,921	75,187	1,631,095	231
t1_niE-2	11,411,515	62	1,191	562,570	10,848,945	3,679,590	1,543,964	252,710	5,372,681	212
t1_niE-3	10,012,344	72	1,507	1,000,811	9,011,533	3,064,588	1,243,462	449,402	4,254,081	465
t1_3D7-iE-1	12,991,483	2	81	850,480	12,141,003	912,334	5,575,569	369,947	5,283,153	233
t1_3D7-iE-2	6,470,351	0	4	225,621	6,244,730	281,177	3,677,882	46,237	2,239,434	240
t1_3D7-iE-3	11,824,305	42	1,023	965,079	10,859,226	3,529,982	1,986,414	392,862	4,949,968	256
t1_ePCR-iE-1	5,571,743	8	60	1450,083	4,121,660	585,628	982,702	215,775	2,337,555	363
t1_ePCR-iE-2	2,366,064	12	215	591,454	1,774,610	434,035	137,804	201,756	1,001,015	122
t1_ePCR-iE-3	6,400,097	12	387	651,993	5,748,104	1,148,564	1,398,684	322,921	2,877,935	181
t24_niE-1	33,411,780	61	1,326	5,688,689	27,723,091	5,762,892	4,456,704	2,896,826	14,606,669	157
t24_niE-2	10,227,177	37	881	899,113	9,328,064	3,242,238	1,646,379	328,760	4,110,687	137
t24_niE-3	6,482,702	2	28	203,593	6,279,109	347,523	4,011,059	58,043	1,862,484	119
t24_3D7-iE-1	14,668,936	0	51	730,638	13,938,298	663,276	7,270,210	498,805	5,506,007	101
t24_3D7-iE-2	5,034,919	0	7	156,980	4,877,939	208,106	2,998,788	161,344	1,509,701	146
t24_3D7-iE-3	57,868,438	377	9,448	5,474,274	52,394,164	16,356,374	8,786,690	2,280,235	24,970,865	230
t24_ePCR-iE-1	6,163,503	2	2	156,258	6,007,245	212,547	3,808,455	92,989	1,893,254	120
t24_ePCR-iE-2	7,262,082	46	916	1,057,919	6,204,163	2,149,075	896,948	293,743	2,864,397	223
t24_ePCR-iE-3	4,907,246	1	6	246,902	4,660,344	336,305	2,697,248	52,875	1,573,916	118

*ePCR-iE, cytoadherent *P. falciparum*−infected erythrocyte; miRNA, microRNA; niE, noninfected erythrocyte, 3D7-iE, non-cytoadherent *P. falciparum*−infected erythrocyte

Appendix Table 2. MicroRNAs differentially expressed in cell-conditioned media of human brain endothelial cells were exposed to niE and compared with ePCR-iE after 1 h incubation*

miRNA	baseMean	log2FoldChange	padj
hsa-miR-150–5p	3628.925319	7.106957417	2.20E-64
hsa-miR-1246	8513.8312	6.854156394	2.86E-33
hsa-miR-342–3p	663.0033186	5.589928255	2.74E-29
hsa-miR-1290	958.7797602	6.480019242	3.64E-22
hsa-miR-223–5p	359.7886812	6.949480635	3.31E-19
hsa-miR-4791	186.7263031	9.764657543	1.81E-13
hsa-miR-143–3p	3014.137094	4.242367581	1.25E-12
hsa-miR-3690	70.86488948	9.209904393	3.00E-12
hsa-miR-145–5p	72.96215294	8.781293485	4.09E-12
hsa-miR-146b-5p	572.9246948	3.850563079	7.29E-12
hsa-miR-150–3p	60.38153154	7.465472022	4.02E-11
hsa-miR-223–3p	3583.963415	10.60183039	6.42E-11
hsa-miR-197–3p	1848.704656	3.167278515	3.68E-10
hsa-miR-6842–3p	121.4605639	5.034134649	3.78E-10
hsa-miR-27a-5p	159.1304428	4.762393491	2.69E-09
hsa-miR-4286	28.41313356	7.592582565	5.34E-09
hsa-miR-4732–3p	39.85412873	−4.344998011	9.19E-09
hsa-miR-29a-3p	264.2422459	3.036225197	3.23E-08
hsa-miR-23a-3p	1648.646951	2.426234941	5.38E-08
hsa-miR-1291	24.09578022	7.678294911	6.73E-08
hsa-miR-140–3p	6094.803676	2.906210556	8.46E-08
hsa-miR-361–3p	518.887784	2.698437793	9.62E-08
hsa-miR-582–3p	45.25401955	5.187956688	1.71E-07
hsa-miR-363–3p	412.4688189	−2.480558611	2.01E-07
hsa-miR-1299	102.3727512	4.139411714	2.36E-07
hsa-miR-28–3p	1018.820725	2.668213456	5.27E-07
hsa-miR-766–3p	29.59956282	5.9824388	5.65E-07
hsa-miR-146b-3p	27.95214056	5.751583995	6.65E-07
hsa-miR-146a-5p	395.7308176	2.295825898	1.07E-06
hsa-miR-486–3p	442.3385331	−2.280314186	1.42E-06
hsa-miR-199b-5p	17.69789788	6.652284259	1.65E-06
hsa-miR-148a-3p	21311.06097	2.967223068	2.14E-06
hsa-miR-769–5p	78.16221633	3.454304058	2.22E-06
hsa-miR-132–3p	13.41828033	6.795969882	2.82E-06
hsa-miR-504–5p	16.20689324	6.842868855	3.34E-06
hsa-miR-92a-3p	65823.55513	−2.10142854	4.67E-06
hsa-miR-330–3p	53.90163431	3.129351136	4.88E-06
hsa-miR-200c-3p	15.27230031	6.716323846	5.34E-06
hsa-miR-486–5p	186570.8541	−2.309900141	5.98E-06
hsa-miR-338–5p	16.14897785	6.511596255	7.43E-06
hsa-miR-183–5p	757.7566497	−2.260214693	7.87E-06
hsa-miR-1273h-5p	11.10031853	6.530890359	1.55E-05
hsa-miR-342–5p	93.52411001	3.308610483	4.55E-05
hsa-miR-326	16.42493563	5.988631002	4.61E-05
hsa-miR-618	15.6716072	6.016209684	4.61E-05
hsa-miR-191–5p	2983.128623	1.523838499	7.79E-05
hsa-miR-27a-3p	285.7014296	1.731405393	7.96E-05
hsa-miR-328–3p	271.7224572	2.170776673	7.96E-05
hsa-miR-451a	14357.385	−1.83622576	9.53E-05
hsa-miR-3614–5p	9.33818402	6.123669779	0.000106957
hsa-miR-30e-3p	815.6225605	2.360699038	0.000125365
hsa-miR-3653–3p	9.955406247	6.067314627	0.000138372
hsa-miR-16–2-3p	99.02227371	−2.704373872	0.000138392
hsa-miR-941	1372.569505	2.112993367	0.000155687
hsa-miR-1273h-3p	8.79013326	5.927996135	0.000189765
hsa-miR-584–5p	74.74437394	−2.177917358	0.000200673
hsa-miR-361–5p	31.19551383	3.652271942	0.000286557
hsa-miR-423–5p	9496.481452	−1.666500408	0.000301254
hsa-miR-425–3p	23.4899942	3.50770916	0.000497233
hsa-miR-1908–5p	5.40110314	−6.802848578	0.000500329
hsa-miR-144–5p	73.08790204	−2.608545423	0.000614181
hsa-miR-148a-5p	7.077958372	5.991607608	0.000826919
hsa-miR-3960	21.82641113	−3.014306593	0.000826919
hsa-miR-92b-3p	284.8388438	−1.662148164	0.001252142
hsa-miR-625–3p	147.3917485	2.170185206	0.001322084
hsa-miR-320a	3462.527306	−1.402939938	0.00139293
hsa-miR-345–5p	22.71828536	3.943197206	0.00139293

miRNA	baseMean	log2FoldChange	padj
hsa-miR-1260a	50.29735001	2.615764632	0.001605391
hsa-let-7i-5p	12361.71358	−1.302787012	0.001797592
hsa-miR-619–5p	22.7811983	3.161529188	0.001900387
hsa-miR-122–5p	3385.264898	−1.584467253	0.002340813
hsa-miR-340–5p	46.36446243	2.653771404	0.002544196
hsa-miR-144–3p	48.36612972	−2.49500384	0.002555714
hsa-miR-126–3p	892.3500608	−1.625098791	0.003126621
hsa-miR-543	129.0107724	−1.784228026	0.003228785
hsa-miR-22–3p	198.2421283	−1.339256703	0.003317174
hsa-miR-125a-3p	25.61739412	2.647707932	0.0045958
hsa-miR-26b-3p	5.972701619	5.518835758	0.0045958
hsa-miR-365a-3p	53.55418216	2.123552072	0.0045958
hsa-miR-365b-3p	53.55418216	2.123552072	0.0045958
hsa-let-7b-5p	11122.0756	−1.385051301	0.004654547
hsa-miR-340–3p	9.403598252	4.19564441	0.007285806
hsa-miR-3158–3p	143.2936325	−1.487178473	0.00782372
hsa-miR-3909	4.660678895	5.033669701	0.008065745
hsa-miR-505–3p	19.61789922	3.184975964	0.009512761
hsa-miR-96–5p	6.228218724	−4.412956083	0.01160297
hsa-miR-92b-5p	15.60484631	−2.774216268	0.011905118
hsa-miR-5684	14.25740308	−3.392469579	0.012209695
hsa-miR-574–3p	151.5421548	1.44861864	0.012209695
hsa-miR-589–5p	112.3400591	1.712421621	0.012209695
hsa-miR-1260b	38.28153971	1.901084012	0.015737938
hsa-miR-17–5p	56.12478112	−1.912960954	0.017636633
hsa-miR-4488	301.3772581	1.686545438	0.019800269
hsa-miR-3150b-3p	9.284489454	3.713227496	0.020280067
hsa-miR-503–5p	39.07218516	−1.757011842	0.023641179
hsa-miR-24–2-5p	7.48136792	3.967586096	0.024393346
hsa-miR-4508	74.78488456	−1.444481229	0.024393346
hsa-miR-193a-5p	184.9649622	1.410027061	0.025848637
hsa-miR-148b-3p	604.5039106	1.071494091	0.025962098
hsa-miR-24–3p	347.9262528	1.011562924	0.025962098
hsa-miR-26a-5p	2978.105792	1.023914595	0.030449772
hsa-let-7a-5p	14867.14987	−1.186931323	0.032443997
hsa-miR-1180–3p	56.26387509	−1.461006415	0.032443997
hsa-miR-128–3p	443.1001246	1.234565868	0.032663654
hsa-miR-4732–5p	37.4933489	−1.669985619	0.033292936
hsa-miR-194–5p	19.87025713	−2.652995088	0.035040129
hsa-let-7e-5p	315.5665007	−1.266168593	0.036277702
hsa-miR-222–3p	1950.75622	−1.054430196	0.04170154
hsa-miR-744–5p	307.4576353	1.101237911	0.04395607
hsa-miR-93–3p	19.14613315	2.21447109	0.04444623
hsa-miR-28–5p	15.19613321	2.619036378	0.047605172

*Positive FoldChange indicates overexpression in niE. RNA sequencing data included a total of 363 microRNAs. baseMean is the mean normalized expression of the miRNAs in all the samples; padj is adjusted for multiple testing by the Benjamini-Hochberg method. ePCR-iE, adherent FCR3 expression endothelial receptor of protein C-infected erythrocytes; miRNA, microRNA; niE, noninfected erythrocytes.

Appendix Table 3. MicroRNAs differentially expressed in cell-conditioned media of human brain endothelial cells when exposed to 3D7-iE and compared with ePCR-iE after 1 h incubation*

miRNA	baseMean	log2FoldChange	padj
hsa-miR-150–5p	3628.925319	6.447621237	8.41E-53
hsa-miR-1246	8513.8312	6.448500505	2.44E-29
hsa-miR-342–3p	663.0033186	4.805719054	1.87E-21
hsa-miR-1290	958.7797602	6.047501723	3.28E-19
hsa-miR-143–3p	3014.137094	4.973540967	3.06E-17
hsa-miR-223–5p	359.7886812	6.431781207	1.96E-16
hsa-miR-4791	186.7263031	10.38932761	2.56E-15
hsa-miR-145–5p	72.96215294	8.773111499	5.33E-12
hsa-miR-23a-3p	1648.646951	2.919080408	3.83E-11
hsa-miR-146b-5p	572.9246948	3.720217317	5.04E-11
hsa-miR-423–5p	9496.481452	−2.845800299	1.45E-10
hsa-miR-223–3p	3583.963415	10.40824443	1.77E-10
hsa-miR-28–3p	1018.820725	3.236927509	7.54E-10
hsa-miR-197–3p	1848.704656	3.045327492	2.21E-09
hsa-miR-3690	70.86488948	7.939040485	3.04E-09
hsa-miR-363–3p	412.4688189	−2.752949366	7.66E-09
hsa-miR-451a	14357.385	−2.623190083	1.10E-08
hsa-miR-4732–3p	39.85412873	−4.446862598	1.22E-08
hsa-miR-4286	28.41313356	7.221117949	3.72E-08
hsa-miR-1299	102.3727512	4.296659106	8.94E-08
hsa-miR-146a-5p	395.7308176	2.416585365	3.27E-07
hsa-miR-320a	3462.527306	−2.147110555	4.06E-07
hsa-miR-150–3p	60.38153154	5.841471731	5.53E-07
hsa-miR-3158–3p	143.2936325	−2.671376413	6.03E-07
hsa-miR-199b-5p	17.69789788	6.756414418	1.41E-06
hsa-miR-326	16.42493563	7.000378659	1.46E-06
hsa-miR-92a-3p	65823.55513	−2.206241834	1.80E-06
hsa-miR-618	15.6716072	6.882512894	2.54E-06
hsa-miR-27a-5p	159.1304428	3.853017578	2.61E-06
hsa-miR-361–5p	31.19551383	4.557109213	3.99E-06
hsa-miR-766–3p	29.59956282	5.475435141	7.17E-06
hsa-miR-338–5p	16.14897785	6.585842515	7.56E-06
hsa-miR-1180–3p	56.26387509	−2.865258808	1.15E-05
hsa-miR-486–5p	186570.8541	−2.257048303	1.36E-05
hsa-miR-486–3p	442.3385331	−2.077360932	1.53E-05
hsa-miR-140–3p	6094.803676	2.378049094	1.89E-05
hsa-miR-1291	24.09578022	6.218174392	2.27E-05
hsa-miR-29a-3p	264.2422459	2.377846317	2.52E-05
hsa-miR-4508	74.78488456	−2.537316275	3.24E-05
hsa-miR-6842–3p	121.4605639	3.458457239	3.89E-05
hsa-miR-200c-3p	15.27230031	6.110652566	5.42E-05
hsa-miR-504–5p	16.20689324	6.10449083	5.42E-05
hsa-miR-582–3p	45.25401955	4.02067135	9.79E-05
hsa-miR-769–5p	78.16221633	2.900427661	0.000122239
hsa-miR-27a-3p	285.7014296	1.699710038	0.000132728
hsa-miR-625–3p	147.3917485	2.549490741	0.000132728
hsa-miR-340–5p	46.36446243	3.201883577	0.000214609
hsa-miR-144–3p	48.36612972	−3.0660485	0.000220627
hsa-miR-425–3p	23.4899942	3.724522238	0.000223367
hsa-miR-320b	420.1406035	−1.862313231	0.000276457
hsa-miR-365a-3p	53.55418216	2.655154806	0.000276457
hsa-miR-365b-3p	53.55418216	2.655154806	0.000276457
hsa-miR-132–3p	13.41828033	5.410556286	0.000380553
hsa-let-7i-5p	12361.71358	−1.47141141	0.000382512
hsa-miR-30e-3p	815.6225605	2.226049992	0.000382512
hsa-miR-92b-5p	15.60484631	−4.163857943	0.0003924
hsa-miR-146b-3p	27.95214056	4.242630881	0.000482005
hsa-miR-92b-3p	284.8388438	−1.785328471	0.000505668
hsa-miR-4732–5p	37.4933489	−2.594968757	0.000643162
hsa-miR-122–5p	3385.264898	−1.753744088	0.000704175
hsa-miR-144–5p	73.08790204	−2.558810315	0.00089817
hsa-miR-3653–3p	9.955406247	5.420823215	0.000963768
hsa-miR-330–3p	53.90163431	2.33736255	0.001216256
hsa-miR-2115–3p	6.041154984	5.834660721	0.001395787
hsa-miR-183–5p	757.7566497	−1.689145385	0.001439809
hsa-miR-1273h-3p	8.79013326	5.232979185	0.001476418
hsa-miR-1273h-5p	11.10031853	5.004655278	0.001837808

miRNA	baseMean	log2FoldChange	padj
hsa-miR-345–5p	22.71828536	3.888926893	0.001844401
hsa-miR-361–3p	518.887784	1.669833063	0.001878529
hsa-miR-328–3p	271.7224572	1.756856697	0.002066471
hsa-miR-3614–5p	9.33818402	5.084630328	0.002066471
hsa-miR-1260a	50.29735001	2.56883531	0.002146885
hsa-miR-191–5p	2983.128623	1.22004135	0.002216696
hsa-miR-505–3p	19.61789922	3.426913927	0.00528521
hsa-miR-4685–3p	26.37952361	−2.212963535	0.006078573
hsa-miR-148a-3p	21311.06097	1.831991607	0.006860876
hsa-miR-126–3p	892.3500608	−1.523444179	0.007103832
hsa-let-7b-5p	11122.0756	−1.342668008	0.007601427
hsa-miR-5189–5p	4.690302347	−6.195706422	0.008125759
hsa-miR-4448	19.99074734	2.751420355	0.008596921
hsa-miR-28–5p	15.19613321	3.329553964	0.008697526
hsa-miR-619–5p	22.7811983	2.721712643	0.011008689
hsa-miR-5684	14.25740308	−3.504790338	0.011818106
hsa-miR-221–5p	30.33237403	2.235527273	0.014993794
hsa-miR-24–3p	347.9262528	1.101827408	0.015833224
hsa-miR-193a-5p	184.9649622	1.491052572	0.020130112
hsa-miR-22–3p	198.2421283	−1.113442482	0.021327869
hsa-miR-93–3p	19.14613315	2.52716344	0.021327869
hsa-miR-2110	117.7715931	−1.410612056	0.02301949
hsa-miR-342–5p	93.52411001	2.045398548	0.02301949
hsa-miR-543	129.0107724	−1.437070341	0.02604373
hsa-miR-155–5p	135.1369051	1.308204109	0.02781228
hsa-miR-152–3p	52.85362465	1.703147513	0.027818637
hsa-miR-584–5p	74.74437394	−1.39071939	0.029085671
hsa-let-7e-5p	315.5665007	−1.333615616	0.030343738
hsa-miR-1908–5p	5.40110314	−4.518938959	0.033717462
hsa-miR-16–2-3p	99.02227371	−1.642902948	0.035497673
hsa-miR-3150b-3p	9.284489454	3.477104992	0.037288673
hsa-miR-106a-5p	5.273323169	−4.723234986	0.046728731
hsa-miR-15b-5p	59.88239009	1.339085366	0.048947187

*Positive FoldChange indicates overexpression in 3D7-iE. RNA sequencing data included a total of 363 microRNAs. baseMean is the mean normalized expression of the miRNAs in all the samples. padj is adjusted for multiple testing by the Benjamini-Hochberg method. ePCR-iE, adherent FCR3 expression endothelial receptor of protein C-infected erythrocytes; 3D7-iE, nonadherent 3D7-infected erythrocytes; miRNA, microRNA.

Appendix Table 4: Characteristics of different miRNAs detected in plasma from children recruited in 2006 for study of malaria, Mozambique

Sample	Total reads	Quality filtered	Complexity filtered	Length filtered	Good-quality reads	rRNA	tRNA	miRNA	Unknown	Different miRNAs
525881.3	10,711,219	1,019	496	3,093,606	7,617,613	1,831,500	651,064	807,691	4,327,358	395
525884.4	13,220,660	803	702	3,888,349	9,332,311	966,969	596,303	1,966,978	5,802,061	574
525885.1	10,702,582	333	566	2,319,260	8,383,322	1,232,736	1,136,730	1,751,858	4,261,998	548
525887.5	13,661,026	1,124	53	2,762,425	10,898,601	594,196	670,121	2,832,128	6,802,156	539
525889.9	26,426,632	1,073	384	2,617,714	23,808,918	2,136,483	2,578,042	5,776,301	13,318,092	642
525891.2	9,524,995	439	270	1,873,951	7,651,044	699,777	854,636	1,589,401	4,507,230	593
525893.6	2,162,887	79	49	120,186	2,042,701	127,077	390,794	440,733	1,084,097	331
525896.7	17,421,782	1,908	548	5,626,333	11,795,449	1,265,772	839,750	1,030,609	8,659,318	341
525898.1	3,320,188	126	118	832,015	2,488,173	142,443	215,289	1,663,216	467,225	425
525899.8	5,937,637	296	454	1,500,015	4,437,622	572,501	700,764	517,740	2,646,617	355
525903.0	14,957,552	2	276	2,265,449	12,692,103	1,692,270	3,040,674	1,194,073	6,765,086	292
525909.2	10,293,853	2,128	224	3,483,287	6,810,566	768,196	599,146	1,269,410	4,173,814	412
544393.2	9,208,074	489	675	2,151,722	7,056,352	1,496,125	1,507,206	883,567	3,169,454	501
544394.9	13,598,660	996	1,250	6,286,338	7,312,322	1,247,933	758,898	1,477,246	3,828,245	580
544395.6	16,309,029	973	1,449	3,847,507	12,461,522	3,653,367	2,378,483	1,189,219	5,240,453	554
544396.3	7,566,573	276	197	1,246,660	6,319,913	627,080	1,632,315	1,027,308	3,033,210	531
544397.0	6,772,398	266	222	1,805,393	4,967,005	1,187,429	550,612	675,373	2,553,591	498
544404.3	7,386,300	287	354	1,583,391	5,802,909	433,117	555,473	996,837	3,817,482	581
544406.7	575,642	0	1	94,684	480,958	34,498	156,803	223,001	66,656	337
544407.4	322,699	7	47	33,711	288,988	26,869	86,815	40,357	134,947	199
544408.1	10,702,037	390	839	2,161,657	8,540,380	710,955	2,179,306	1,632,353	4,017,766	663
544413.5	15,424,105	20	208	3,016,358	12,407,747	2,130,079	1,918,422	2,473,544	5,885,702	276
544415.9	15,845,270	581	585	4,355,557	11,489,713	1,693,453	1,942,665	3,572,255	4,281,340	757
544417.3	320,995	6	47	49,727	271,268	79,124	58,275	53,365	80,504	229
544423.4	12,314,227	511	879	2,620,234	9,693,993	1,146,777	1,257,197	2,022,726	5,267,293	620
544425.8	6,960,365	244	319	1,393,757	5,566,608	452,538	1,278,619	967,048	2,868,403	473
544430.2	29,411,214	2,681	2,251	7,142,325	22,268,889	2,330,062	2,430,827	2,447,114	15,060,886	472
544431.9	12,913,067	374	771	2,019,212	10,893,855	1,553,982	2,423,487	2,087,189	4,829,197	298
544434.0	9,194,679	428	55	1,158,428	8,036,251	1,187,467	1,514,795	1,642,793	3,691,196	433
544436.4	10,628,594	352	242	1,424,162	9,204,432	1,030,961	2,030,035	2,940,439	3,202,997	465
544439.5	18,820,329	990	1,239	3,728,346	15,091,983	1,867,354	2,041,446	1,558,034	9,625,149	659
566322.2	9,096,499	219	526	970,253	8,126,246	222,824	1,176,992	1,440,172	5,286,258	463
566323.9	12,512,273	307	147	681,565	11,830,708	373,103	468,855	8,338,268	2,650,482	770
566324.6	7,407,842	271	230	799,057	6,608,785	473,056	1,541,802	2,306,487	2,287,440	644
566327.7	265,530	5	26	39,505	226,025	23,941	18,230	86,877	96,977	274
566329.1	575,470	7	48	23,763	551,707	59,080	163,228	133,556	195,843	311
566332.1	9,282,984	18	577	2,188,722	7,094,262	936,251	1,105,618	2,509,571	2,542,822	310
566333.8	12,485,750	1,976	85	3,068,214	9,417,536	1,147,898	945,883	1,973,103	5,350,652	669
566335.2	16,300,010	1,628	450	3,430,462	12,869,548	1,439,268	1,267,034	2,367,655	7,795,591	395
566353.6	12,299,560	520	92	4,379,950	7,919,610	1,052,903	619,183	2,088,724	4,158,800	612
566355.0	2,968,770	0	79	1,009,357	1,959,413	328,104	255,943	440,443	934,923	160
566356.7	15,403,237	1,053	1,726	3,642,172	11,761,065	2,419,028	1,509,598	1,633,826	6,198,613	628
566358.1	8,943,757	529	1,773	3,677,028	5,266,729	1,105,767	487,154	1,637,474	2,036,334	454
566359.8	744,578	20	72	58,563	686,015	35,746	148,801	79,994	421,474	288
566361.1	25,792,113	905	1,378	7,723,560	18,068,553	1,793,988	2,690,970	6,727,806	6,855,789	580
566362.8	12,021,808	747	24	3,274,341	8,747,467	1,603,501	18,940	10,773	7,114,253	151

Sample	Total reads	Quality filtered	Complexity filtered	Length filtered	Good-quality reads	rRNA	tRNA	miRNA	Unknown	Different miRNAs
566364.2	1,631,464	99	104	556,133	1,075,331	112,855	251,575	48,887	662,014	274
566365.9	19,129,131	2	966	1,691,465	17,437,666	2,087,295	2,389,159	7,624,018	5,337,194	399
566366.6	19,623,668	7,037	92	5,322,923	14,300,745	1,231,391	1,029,852	1,170,845	10,868,657	467
566367.3	384,010	3	32	97,518	286,492	22,854	26,912	122,521	114,205	150
579033.4	12,761,288	299	223	2,438,291	10,322,997	4,471,210	1,076,958	2,371,736	2,403,093	570
579034.1	7,225,891	25	2,766	472,409	6,753,482	472,354	2,250,034	994,990	3,036,104	465
579035.8	9,863,866	517	265	2,370,430	7,493,436	441,043	567,999	1,734,312	4,750,082	481
579036.5	145,356	0	13	17,436	127,920	4,210	11,235	65,688	46,787	196
579037.2	1,493,408	4	82	338,939	1,154,469	47,182	229,698	521,844	355,745	394
579038.9	10,367,363	371	1,380	3,078,000	7,289,363	639,425	1,550,985	991,123	4,107,830	388
579040.2	9,253,151	13	408	2,472,738	6,780,413	384,449	1,761,922	500,022	4,134,020	373
579042.6	15,960,129	470	202	2,728,371	13,231,758	638,919	3,805,700	1,934,893	6,852,246	380
579043.3	7,089,342	206	697	1,602,007	5,487,335	964,876	1,536,510	687,802	2,298,147	260
579045.7	1,982,823	2	433	143,776	1,839,047	233,623	490,286	324,346	790,792	305
579046.4	1,873,456	486	38	806,002	1,067,454	75,715	60,748	43,809	887,182	185
579048.8	1,082,686	1	50	185,056	897,630	54,474	153,016	135,343	554,797	200
579050.1	170,063	2	27	17,739	152,324	17,255	29,933	23,521	81,615	160
579051.8	10,722,970	448	158	1,708,024	9,014,946	642,574	2,552,986	1,186,376	4,633,010	313
579052.5	4,228,866	219	748	2,256,487	1,972,379	246,201	433,194	222,570	1,070,414	146
579053.2	8,618,384	462	1,092	1,949,499	6,668,885	354,969	1,025,766	994,142	4,294,008	319
579054.9	9,386,303	689	143	4,284,092	5,102,211	340,702	1,452,895	638,954	2,669,660	242
579055.6	3,526,717	94	80	1,769,909	1,756,808	199,283	294,707	223,967	1,038,851	123
579058.7	1,792,508	133	10	997,704	794,804	53,040	154,970	126,036	460,758	242
579059.4	17,665,599	8	910	1,746,197	15,919,402	1,020,271	3,146,816	6,390,514	5,361,801	365
579060.0	11,438,101	537	771	3,749,312	7,688,789	618,651	1,015,852	548,212	5,506,074	300
579061.7	33,311,564	3	1,496	2,576,915	30,734,649	2,601,559	5,795,176	11,096,716	11,241,198	442
579062.4	3,451,830	156	2	1,762,819	1,689,011	202,947	239,684	218,299	1,028,081	116
579064.8	8,994,815	278	178	2,721,236	6,273,579	840,779	987,181	593,171	3,852,448	161
579065.5	18,176,617	7,425	386	6,172,449	12,004,168	781,469	399,288	948,897	9,874,514	334
579068.6	5,128,830	305	256	1,520,699	3,608,131	300,353	890,927	810,364	1,606,487	396
579069.3	45,577,321	37	4,302	2,027,990	43,549,331	926,339	3,622,063	5,903,995	33,096,934	786
579075.4	9,827,499	20	816	1,032,689	8,794,810	363,164	665,426	1,692,835	6,073,385	515
579077.8	10,214,090	344	167	1,093,407	9,120,683	1,504,424	989,870	3,501,517	3,124,872	595
579078.5	4,481,826	234	167	2,157,860	2,323,966	119,110	242,195	281,184	1,681,477	175
579079.2	1,225,321	30	72	869,796	355,525	78,232	60,481	95,781	121,031	204
598991.0	8,703,408	2	406	1,378,261	7,325,147	439,304	989,308	2,636,136	3,260,399	546
598993.4	7,424,401	473	236	3,018,779	4,405,622	292,897	603,224	430,567	3,078,934	181

Appendix Table 5. Spearman correlations between ELISA-based HRP2 levels and miRNA relative expression levels (RELs) in plasma samples from children with malaria, Mozambique*

miRNA	rho	p value
Children recruited in 2006		
hsa-miR-10b-5p	0.415	0.020
hsa-miR-378a-3p	0.422	0.020
hsa-miR-4497	0.533	<0.001
Children recruited in 2014		
hsa-miR-122–5p	−0.016	0.892
hsa-miR-320a	0.121	0.320
hsa-miR-1246	0.066	0.588
hsa-miR-1290	0.123	0.310
hsa-miR-3158–3p	0.511	<0.001
hsa-miR-4497	0.401	<0.001

*HRP2 levels and miRNA RELs were log transformed.

Appendix Table 6. PCR efficiencies of each microRNA used for reverse transcription quantitative PCR analysis of specimens from children with malaria, Mozambique

miRNA	PCR efficiency, %
hsa-miR-122–5p	99.6
hsa-miR-320a	95.3
hsa-miR-1246	98.4
hsa-miR-1290	103.0
hsa-miR-3158–3p	91.2
hsa-miR-4497	96.9
has-miR-191–5p	93.1
hsa-miR-30d-5p	103.8
hsa-miR-148a-3p	100.1
ath-miR-159a	103.2

Appendix Table 7. Predicted targets of the 2 miRNAs (hsa-miR-3158–3p and hsa-miR-4497) validated in children with malaria recruited in 2014, Mozambique

hsa-miR-3158–3p	hsa-miR-4497
TXNIP	RUNX1
MAP3K9	CCNF
ZNF704	CTTN
BCL7A	FANCA
GATAD2B	NAB2
FBXO46	NF2
CHST15	NPY4R
FTSJ3	PRPS1
CTC1	TPM3
CABP7	UGT8
C20orf194	VEGFA
IGSF8	RAB9A
KLHL15	IRX5
NLK	BPNT1
NFASC	APPBP2
LMNB2	CD226
MRPS18A	ATP1B4
LSM4	SH2B1
XRCC6	SDF4
ZBTB39	MTPAP
UBXN2B	TMEM33
RRP7A	DUSP22
ZCCHC14	RAB22A
RANGAP1	TBC1D24
RAB3IP	ZNF490
AMOTL2	DSN1
ANXA11	FBXL18
C22orf39	LRRC27
DDX6	ATP13A4
CDK2	HIST1H2AH
ENAH	SP140L
ENPP5	CAMK2N2

hsa-miR-3158–3p	hsa-miR-4497
GDAP1L1	C10orf71
FOSL1	FAM83C
MMP15	MIPOL1
PLAG1	CCNY
NANOS1	PRPS1L1
MRTO4	CBARP
PIGQ	LHFPL3
NLGN1	C8orf82
RTN2	PPAN-P2RY11
SAMD4A	CASTOR2
PTPRJ	
THSD7A	
ZNF281	

Appendix Table 8. Clustering results of DAVID analysis in study of malaria in children, Mozambique

Category	Term	Genes	Fold enrichment	p value	Benjamini p value
GOTERM_CC_DIRECT	GO:0030687~preribosome, large subunit precursor	PPAN-P2RY11, FTSJ3, MRTO4	25.136	0.006	0.647
GOTERM_BP_DIRECT	GO:0007399~nervous system development	IGSF8, NAB2, VEGFA, NLGN1, BPNT1, PRPS1	4.875	0.007	0.977
GOTERM_CC_DIRECT	GO:0045335~phagocytic vesicle	RAB9A, ANXA11, RAB22A	18.691	0.011	0.605
GOTERM_MF_DIRECT	GO:0000287~magnesium ion binding	NLK, MTPAP, PRPS1L1, BPNT1, PRPS1	5.237	0.015	0.902
GOTERM_BP_DIRECT	GO:0006015~5-phosphoribose 1-diphosphate biosynthetic process	PRPS1L1, PRPS1	116.611	0.017	0.987
GOTERM_BP_DIRECT	GO:0002175~protein localization to paranode region of axon	NFASC, UGT8	116.611	0.017	0.987
GOTERM_BP_DIRECT	GO:0009156~ribonucleoside monophosphate biosynthetic process	PRPS1L1, PRPS1	93.288	0.021	0.974
GOTERM_MF_DIRECT	GO:0004749~ribose phosphate diphosphokinase activity	PRPS1L1, PRPS1	85.473	0.023	0.702
GOTERM_CC_DIRECT	GO:0043231~intracellular membrane-bounded organelle	CTTN, MTPAP, RANGAP1, UGT8, RUNX1, ATP13A4, DDX6	3.048	0.026	0.667
GOTERM_MF_DIRECT	GO:0019003~GDP binding	RAB9A, RAB22A, PRPS1	11.871	0.026	0.641
GOTERM_CC_DIRECT	GO:0005635~nuclear envelope	TMEM33, ANXA11, ATP1B4, RANGAP1	6.112	0.027	0.602
GOTERM_CC_DIRECT	GO:0030027~lamellipodium	ENAH, CTTN, NF2, RAB3IP	6.074	0.027	0.542
GOTERM_BP_DIRECT	GO:0030913~paranodal junction assembly	NFASC, UGT8	66.634	0.029	0.978
GOTERM_CC_DIRECT	GO:0000932~cytoplasmic mRNA processing body	LSM4, SAMD4A, DDX6	9.345	0.04	0.627
GOTERM_MF_DIRECT	GO:0030371~translation repressor activity	NANOS1, SAMD4A	38.851	0.049	0.798
GOTERM_CC_DIRECT	GO:0001726~ruffle	CTTN, NF2, RAB22A	8.099	0.052	0.674
GOTERM_BP_DIRECT	GO:0000956~nuclear-transcribed mRNA catabolic process	LSM4, MRTO4	35.88	0.054	0.996
GOTERM_BP_DIRECT	GO:0033962~cytoplasmic mRNA processing body assembly	LSM4, DDX6	35.88	0.054	0.996
GOTERM_BP_DIRECT	GO:0071425~hematopoietic stem cell proliferation	RUNX1, CTC1	33.317	0.058	0.994
GOTERM_BP_DIRECT	GO:0051301~cell division	DSN1, CCNY, CCNF, ANXA11, CDK2	3.331	0.061	0.99
GOTERM_BP_DIRECT	GO:0009165~nucleotide biosynthetic process	PRPS1L1, PRPS1	31.096	0.062	0.983
GOTERM_CC_DIRECT	GO:0042470~melanosome	RAB9A, TMEM33, ANXA11	7.217	0.063	0.708

Category	Term	Genes	Fold enrichment	p value	Benjamini p value
GOTERM_CC_DIRECT	GO:0005856~cytoskeleton	ENAH, CTTN, NF2, RAB3IP, TPM3	3.274	0.064	0.673
GOTERM_MF_DIRECT	GO:0005161~platelet-derived growth factor receptor binding	PTPRJ, VEGFA	28.491	0.067	0.837
GOTERM_BP_DIRECT	GO:0050860~negative regulation of T cell receptor signaling pathway	PTPRJ, DUSP22	27.437	0.069	0.984
GOTERM_MF_DIRECT	GO:0044822~poly(A) RNA binding	PPAN-P2RY11, RRP7A, XRCC6, ANXA11, MTPAP, LSM4, FTSJ3, SAMD4A, MRTO4, DDX6	1.892	0.075	0.828
GOTERM_BP_DIRECT	GO:0009116~nucleoside metabolic process	PRPS1L1, PRPS1	24.549	0.077	0.984
GOTERM_BP_DIRECT	GO:0051894~positive regulation of focal adhesion assembly	PTPRJ, VEGFA	22.211	0.085	0.985
GOTERM_BP_DIRECT	GO:0000027~ribosomal large subunit assembly	PPAN-P2RY11, MRTO4	22.211	0.085	0.985
GOTERM_CC_DIRECT	GO:0005770~late endosome	RAB9A, RAB22A, SDF4	5.975	0.087	0.757
GOTERM_MF_DIRECT	GO:0019901~protein kinase binding	PTPRJ, FAM83C, CCNY, CAMK2N2, CD226	2.841	0.096	0.862
GOTERM_BP_DIRECT	GO:0007422~peripheral nervous system development	NFASC, UGT8	19.435	0.096	0.987

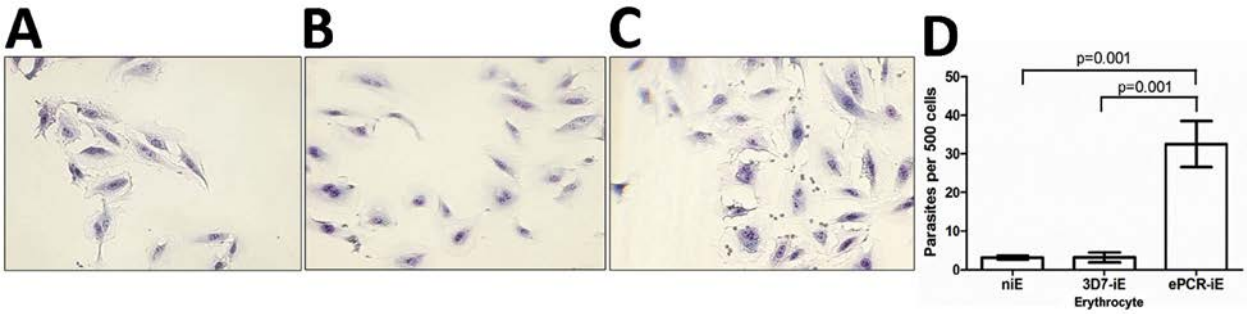

Appendix Figure 1. Cytoadhesion assay of infected erythrocytes (iEs) with human brain endothelial (HBE) cells stained with Giemsa and visualized at original magnification ×200. A) Noninfected erythrocytes (niE). B) Nonadherent 3D7-infected erythrocytes (3D7-iE). C) Adherent FCR3 expression endothelial receptor of protein C-infected erythrocytes (ePCR-iE). D) Comparison of 3 groups of infected and noninfected erythrocytes adhered to HBE cells. Bars represent mean and T lines, SD. p values were calculated by unpaired t-test.

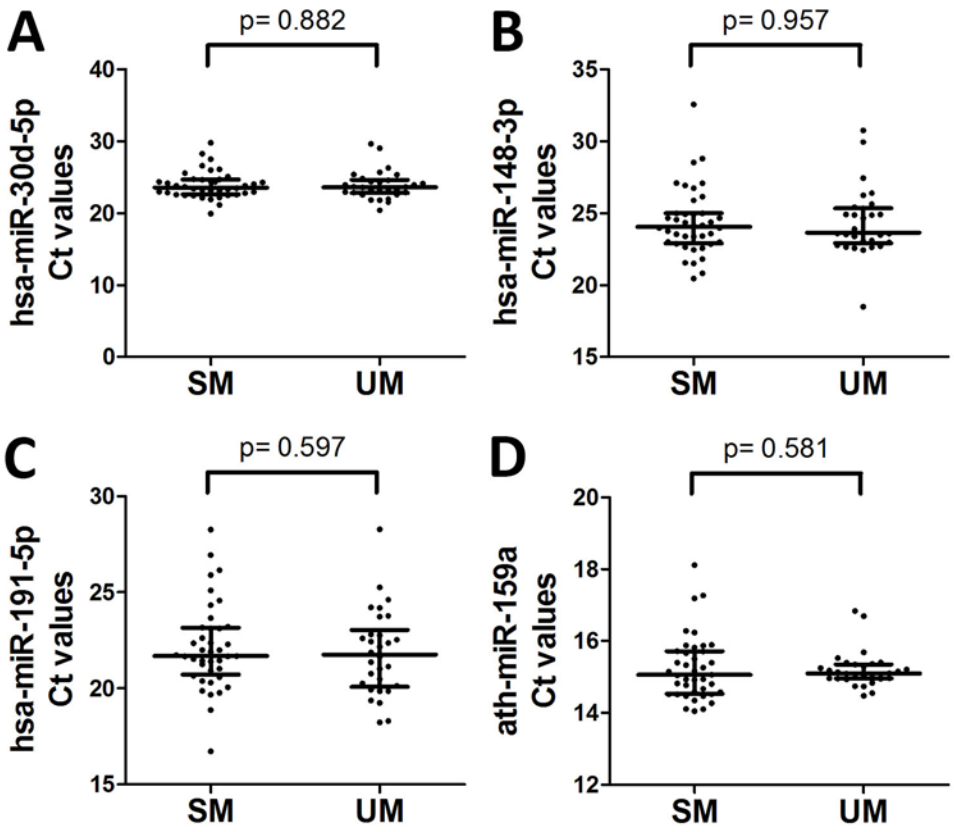

Appendix Figure 2. RT-qPCR C_t values of exogenous (ath-miR-159a) and endogenous (hsa-miR-191–5p, hsa-miR-30d-5p, and hsa-miR-148a-3p) controls in severe malaria (SM) and uncomplicated malaria (UM) groups. Distributions were compared by Mann-Whitney U test. T bars represent median and interquartile Ranges.